Characterization of Antibacterial Fabric Nanocomposites Based on Silver /Copper Oxide and Polymer Blend with Electron Beam Radiation

Hanan. M. Eyssa (Hanan_eyssa@yahoo.com)
Egyptian Atomic Energy Authority
Rawia F. Sadek
Egyptian Atomic Energy Authority
R Attia
Egyptian Atomic Energy Authority

Research Article

Keywords: Cotton fabrics, Ag/CuO/CMC–PEG–EG nanocomposites, Antibacterial activity, Electron beam radiation

Posted Date: June 23rd, 2022

DOI: https://doi.org/10.21203/rs.3.rs-1755126/v1

Abstract

Cotton fabrics are usually used for medical purposes, but they can be damaged when exposed to microorganisms. Through modification with carboxymethyl cellulose–polyethylene glycol–ethylene glycol hydrogel/silver/copper oxide (CMC–PEG–EG/Ag/CuO) nanocomposites and subsequent irradiation using an electron beam accelerator, this study proposes an effective method for avoiding bacterial risks on cotton fabrics. The results showed that cotton fabrics loaded with CMC–PEG–EG/Ag/CuO had a low water vapor permeability (WVP) value of 0.09 (0.006% for Ag and 2% for CuO) at a dose of 5 kGy compared with unloaded cotton fabrics (0.33). The tensile strength of the modified cotton fabrics, which had various formulations, was significantly improved with EB irradiation until 25 kGy, exceeding that of the unloaded fabrics. Thermal stability was enhanced by adding CuO nanoparticles up to 2%. The antibacterial activity of the modified cotton fabrics was analyzed by examining gram-negative and gram-positive bacteria. The results showed that the modified cotton fabrics had the highest inhibition zone effect, with 20 and 15 mm for both gram-negative and gram-positive bacteria, respectively. In addition, CMC–PEG–EGs incorporated with 0.006% Ag and 0.012% CuO irradiated at a dose of 5 kGy and 0.006% Ag and 0.5% CuO at a dose of 25 kGy were the most efficient formulations. Meanwhile, a 0.012% concentration of CuO nanoparticles in the formulation was considered appropriate to provide the best antimicrobial activity, as the cost of modifying the fabrics was minimized.

Introduction

Owing to their ability to afford a great quality lifecycle and safety profits to persons, antimicrobial textiles have attracted much attention from academic research and manufacturing in recent years. Fabric products be situated susceptible to crowd microorganisms responsible for disease, odor, color degradation, and textile deterioration. Antimicrobial fabrics can be used to produce various finished products, such as casual wear, outerwear, underwear, footwear, upholstery, beds, hospital linens, wound repair bandages, different towels, and napkins (Dastjerdi et al., 2010). The use of self-sterilizing textiles can reduce infection transmission among clinic residents and protect biological warfare and other applications. Cotton textiles have a great marketplace share among textile products owing to the excellent nature of cotton, such as elasticity, comfortability, water absorption, and air permeability. However, cotton fabrics can provide a conducive environment for microbial growth (e.g., bacteria and fungi) because they offer moistness, temperature, oxygen, and adequate nutrients (tints, dead skin cells, moisture, other skin excretions, etc.). Bacteriological pathogens that occupy textile surfaces can induce foul odors, fabric deterioration, and probable health dangers. Consequently, antibacterial fabrics are in great demand in the market and have attracted many researchers. Various antibiotic chemicals that contain organic nanoparticles, N-halamines, polybiguanides, chitosan, quaternary ammonium compounds, and triclosan have been used to fortify textile goods, such as bed sheets, sportswear, underwear, whacks, shoe liners, underwear, auto air screens fabrics, and external and medical fabrics (Shahid et al., 2013). Through its practical applications, many problems, including resistance to

microorganisms, environmental hazards, and damage to human health, have been encountered (Xu et al., 2013).

Carboxymethyl cellulose (CMC), a crucial derivative of cellulose, is nontoxic and has great chemical stability. Owing to its great performance in thickening, dispersion, emulsification, and stability, CMC has been widely applied in various fields, such as medicine, the food industry, petroleum, daily chemistry, textile, papermaking, and architecture (Kanikireddy et al., 2020). In this chemical structure, the carboxymethyl group ($-CH_2-COOH$) is attached to the hydroxyl group of the glucopyranose chain in cellulose. However, owing to its reduced antibacterial activity and low mechanical strength, CMC cannot properly act as an actual wound-healing agent. Therefore, synergizing CMC hydrogels and membranes with antibacterial agents and medicines is necessary in order to regulate and maintain the presence of antibacterial agents that prevent microbial growth in injuries and to enhance healthcare quality (Abdollahi et al., 2019).

Biodegradable and biocompatible hydrogels can be formulated using CMC and polyethylene glycol (PEG). PEG can be equipped to act as a physical block to avoid surgical adhesions. PEG is a polyether that is amphiphilic and soluble in water and in many organic solvents (Capanema et al., 2019). The hydrophilic arrangement of PEG can offer extra biocompatibility to structures, and the addition of CMC directly to crosslinkers among polymer chains can produce a compacted structure. It takes hydroxyl groups at the terminal ends of the chain that can be functionalized simply through different functional groups. Owing to this purpose, PEG-based hydrogels have been discovered on a large scale for medicine transfer (Lin & Anseth, 2009). Although several authors have described PEG as hydrophilic, it also exhibits hydrophobicity due to the existence of ethylene groups (Sanad et al., 2021). In addition, maximum PEGs with a molecular weight of less than 1000 g/mol can detach quickly from the body system, necessitating its extensive practice in biomedical applications (Lee et al., 2005). The formulation to be dried or crosslinked via electron beam radiation typically comprises unsaturated monomers (double bonds), oligomers, and supplementary additives, depending on the desired properties. Initial tests revealed that ethylene glycol (EG) as a hydrophilic monomer significantly influences the bonds on cotton textile surfaces, which improves the physical performance of the formulation in terms of elasticity and homogeneity; thus, the corresponding monomer of EG was used (El-Naggar et al., 2005).

Among the ingredients used in this mixture are nanosized metals and metal oxides with a group of cellulose derivatives, which show excellent antibacterial activity and decent mechanical strength (DeBoer et al., 2015). Among the metal nanoparticles or metal oxides used for antimicrobial agents, nano-Ag/CuO are suitable due to the following characteristics: antimicrobial property, photo-oxidation capability against biochemical and biological types, electrical conductivity, and self-sterilization. Nano-Ag/CuO is usually considered a harmless material intended for persons and animals, and it has been widely used to prepare particular care goods (Sanad et al., 2021). Ag/CuO exhibits substantial antibacterial activities after the atom size is abridged to a nanosized scale, and nano-Ag/CuO particle can interrelate with the external bacteria and/or with the bacterial pulp, where it goes inside the prison cell, exhibiting outstanding bactericidal activity (Sanad et al., 2021). Silver nanoparticles (AgNPs) were synthesized in CMC with

cashew resin hydrogels in order to fasten wound healing and antibacterial activity (Lustosa et al., 2017). However, these applications of AgNPs have also encountered problems due to environmentally friendly issues, which are mostly produced by the leakage of Ag ions from antibacterial fabrics (Dahlan et al., 2021).

Radiation has been considered an effective method for developing hydrogels. The irradiation procedure has many advantages: it can be easily controlled, hydrogel formation and disinfection can be linked in one technical stage, and additional initiators and crosslinks, which may be harmful or difficult to eliminate, are not required. Recently, electron beam tools have been used such as an additional green technique aimed at old-style fabric wet treating, particularly superficial modification procedures. Electron beam radiation is dry, pollution-free, and cool equipment that removes the necessary materials used for diluents and components used in wet chemical processes (Elmaaty et al., 2022). EB irradiation has been extensively used in general polymer, compound curation, polymer modification, and fiber surface modification (Thite et al., 2018). This type of radiation can achieve an optimized production of hydrogels. The use of irradiation crosslinked CMC–PEG hydrogels as a barrier to avoid postoperative adhesions has been recognized (Lee et al., 2005).

Some studies have used polymer hydrogels to study and characterize antibacterial cotton fabric composites. Wang et al., (2022) prepared a modified cotton fabric using carboxymethyl chitosan with trimethylammonium chloride and methyl acrylate to improve antibacterial activities. Using fumaric acid as a crosslinking agent, (Bozaci et al., 2015) modified cotton fabrics by dispersing AgNPs in CMC to investigate antimicrobial properties. The poly-N-vinyl-2-pyrrolidone (PVP)-formulated cotton fabric treated with TiO_2 NP-doped Ag showed good antimicrobial activity against gram-negative and gram-positive bacteria and fungi (Hebeish et al., 2013). Khafaga et al., (2015) embedded cotton fabrics into CMC/polyvinyl alcohol hydrogel/TiO_2 nanocomposite solutions, followed by gamma irradiation, to form a crosslinked structure on the cotton cellulose surface to evaluate antimicrobial activity against *E. coli* (Gram-ve) bacteria. (Saleh et al., 2022) studied the antimicrobial activity of cotton and cotton/polyester fabrics through immersion in compounds containing copper/chitosan (Cu/CS) nanocomposites as antimicrobial agents and in poly (vinyl alcohol)/plasticized starch (PVA/PLST) blends with different ratios.

In this study, we synthesized CuO NPs using green chemistry and a sol–gel method, which is applied to cotton textiles, and examined the antimicrobial activity of this modified cotton textile. The effects of CuO concentration and Ag on the antibacterial properties of the modified fabric were examined. In addition, the special effects of treatments on cotton textiles were analyzed by thermogravimetric analysis (TGA), Fourier transform infrared (FTIR) and scanning electron microscope (SEM) analyses. Water vapor permeability (WVP) and tensile strength were also investigated. CMC–PEG–EG/Ag/CuO nanocomposites were equipped and applied to the cotton fabric to develop its antibacterial properties using EB irradiation as a source ray.CMC–PEG–EG/Ag/CuO nanocomposite cotton fabrics were characterized by SEM and FTIR.

Experimental Section

Materials

Plain-weave cotton fabrics were purchased from El-Nasr Company for Spinning, Weaving, and Dyeing, El-Mahalla El-Kubra, Egypt. The cotton fabrics were scoured and not subjected to any further finishing processes. Polyethylene glycol was purchased from Fluka Co., Germany, with an OH Functionality = 2.0, and Mw = 600 g/mol. CMC sodium salts have high viscosity and were bought from El-Nasr Pharmaceutical Chemicals, Egypt, EG from Qualikems Fine Chem Pvt. Ltd., India, and $CuCl_2 \cdot 2H_2O$ (copper chloride dihydrate, 98.0%) from LOBA Chemie Pvt. Ltd., China. Ethanol of laboratory grade was supplied by El-Nasr Pharmaceutical Chemicals, Egypt. AgNPs were prepared according to a previous work (Eyssa et al., 2019). *Moringa* leaves were collected from the Department of Botany, College for Women, Ain-Shams University, Cairo, Egypt. Laboratory-grade agar powder was obtained from Nice Chemicals, India. Pathogenic microorganisms of both gram-negative (*Escherichia coli*) and gram-positive (*Staphylococcus epidermis*) bacteria were obtained from Microbiologics, Inc., Minnesota, USA.

Extract preparation

Plant extract preparation

The collected *Moringa* leaves were washed with faucet water and then deionized water to eliminate undesirable impurities. The leaves were dried at room temperature for preparation purposes. The aqueous leaf extract (1 g) of green *Moringa* was boiled using deionized water for 1 h, filtered using Whatman No.1 filter paper, and stored in the refrigerator. The aqueous extract was used to prepare the CuO NPs.

Copper oxide nanoparticle synthesis

By utilizing green chemistry, a sol–gel method was used to synthesize CuO NPs (**Fig. 1**). Copper oxide dihydrate was dissolved in deionized water, stirred and heated to prepare 0.2 M solution, and the aqueous extract of *Moringa* leaf was then added to copper chloride solution. Subsequently, sodium hydroxide (8 M) was added to the mixture solution until a large amount of precipitate was formed. The color of the solution mixture quickly changed from blue to black, and a black precipitate was obtained. The black precipitate was washed many times using deionized water and was then filtered with drying at 100°C. The calcination process of the precipitate was performed at 500°C for 4 h.

Preparation of CMC–PEG–EG/Ag/CuO nanocomposites

CMC–PEG–EG with a weight of 1.35 g was added in amount from ethanol and deionized water and stirred for 2 h at 80°C until complete miscibility was formed. While stirring, the desired weight of the prepared CuO (0.012, 0.5, 1, and 2%) with Ag (0.006%), according to total volume, was added to the solution as a dispersed phase to realize the required composite.

Application to cotton fabric and EB irradiation

Cotton fabric samples were padded in the CMC–PEG–EG solutions that contained the dispersed Ag/CuO NPs at various concentrations of CuO (0.012, 0.5, 1, and 2%) with 0.006% Ag, squeezed to set the pickup of 100 (%), and then irradiated at various doses. The unmodified and modified cotton fabrics were exposed to EB radiation at room temperature in atmospheric air, utilizing a 2.7 MeV and 25 kW EB accelerator, at a current of 10 mA, installed at the NCRRT (EAEA), Egypt. The irradiation doses used were 5, 10, and 25 kGy.

Characterization of the synthesized CuO NPs

Transmission electron microscopy (TEM)

The particle size and shape of the prepared CuO NPs were measured using a TEM model JEM-2100 with a voltage of 200 kV (JEOL Co., Japan).

Fig.1. Schematic diagram for the preparation of CuO NPs

X-ray diffraction (XRD)

The prepared CuO NPs were investigated using XRD (XRD 6000, Shimadzu Instruments). The XRD patterns from 4°–90° were performed at a scan rate of 2 °/min on a diffractometer with Cu Kα radiation (40 mA generator current, 40 kV generator voltage, and λ = 0.15406 nm) at ambient temperature.

Energy dispersive X-ray (EDX) and mapping image analysis

EDX was utilized to determine the elemental composition and mapping images of the CuO NPs and was performed using an EDX unit (SmartEDX Company, UK).

Characterization of the modified cotton fabric

Morphological analysis

A scanning electron microscope (SEM; ZEISS EVO 15 SEM, UK) was utilized to characterize the CuO NP powder and the fracture morphology of the prepared samples CMC–PEG-EG/Ag/CuO (0.012, 0.5, 1, and 2% CuO NPs) on the cotton fabrics.

Fourier transform infrared (FTIR) spectroscopy

The infrared spectra were carried out to examine the nanocomposites using an FTIR spectrometer (Vertex 70 Bruker Optics, Germany) with a resolution of 4 cm^{-1} to software 64 scans and within a wide wavenumber range 400–4000 cm^{-1}. The spectrometer was equipped with an attenuated total reflectance (ATR) unit to test the ATR spectra of the characterized samples at ambient temperature.

Determination of crosslinking density

The real stress (σ) in simple dilation can be taken as a total of twain contributions (Eyssa et al., 2021):

$$\sigma = \sigma_{o}\left(\lambda\right) + Ge(\lambda^{2} - \frac{1}{\lambda})$$

1

,

where σ is the real stress, which equals the titular stress multiplied by the expansion ratio k, σo depends on the chemical nature of the polymer, and Ge is the curve slope, which is linked to the crosslinking degree and can be determined by plotting σ versus $\lambda^{2} - \lambda^{-1}$. The average molecular weight between crosslinks (Mc), which is directly attached to the crosslinking density, can be evaluated from the Ge value using Eq. (2), based on Zang et al. (Zang et al., 1989).

$$Mc = A\ \delta RT/Ge,$$

2

where the prefactor A is presumed to be 1, R is the gas fixed constant (8,314,463 cm^{3} Pa K^{-1} mol^{-1}), T is the temperature, and δ is the density of the specimen.

The crosslinking density can be determined from the Mc amount, as follows:

Crosslinking density (v) = $1/2Mc$ (3)

Mechanical property measurements

The mechanical parameters were determined at ambient temperature (25°C ± 2°C), based on the ASTM D5034 for textile fabrics. Dimensions of quadrangular specimens at 50 × 100 mm were tested. Tenile strength and elongation at break were measured at a crosshead speed of 70 mm/min on a Qchida computerized tensile testing machine (Dongguan Haida Equipment Co. Ltd., China). The average value of the tested mechanical parameters was obtained by examining at least three samples.

Water vapor permeability (WVP)

The WVP was dignified in agreement with the standard AS-2001.2.34:1990. A fixed volume of distilled water was put in a conical flask, which was tightly sealed with the tested fabrics. The test was done at room temperature for 24 h and at a temperature of 70°C for 2 h using an oven. The experiment was conducted ten times at a pressure of 100 kPa, and a tube no-04 (L/min) using a minor opening diameter of 2.8 cm.

TGA measurements

The thermal stability of modified cotton fabrics was estimated via TGA utilizing a TGA-50 instrument (Shimadzu, Japan) at a heating rate of 10°C/min under nitrogen gas atmosphere from room temperature to 600°C, with a flow rate of 20 mL/min. The specimen weights were between 2 and 5 mg.

Evaluation of the antimicrobial properties of the coated fabrics

Antibacterial qualitative agar diffusion method

A disk diffusion test was performed according to (Selvarani et al. 2013) to study the antibacterial activity of the tested nanoparticles (Ag and CuO) and to identify the bacterial activity by measuring the surrounding inhibition zone for the modified samples. From each isolate, 1 ml broth cultures of gram-positive (*Staphylococcus epidermis*) and gram-negative (*Escherichia coli*) containing (4 × 106 CFU/mL) were swabbed over the surface of the Mueller–Hinton agar plate using a sterile cotton swab. The unmodified (control) and modified cotton fabrics were cut into small pieces (1 cm^2) and gently pressed onto the swabbed agar surface. The plates were incubated at 37°C for 24 h. The susceptibility of tested microorganisms was determined by measuring the surrounding area of the inhibition zone.

Results And Discussion

The prepared CuO NP evaluation

The CuO structure was examined using XRD (**Fig. 2**). Observably, the highest two peaks of 2θ at 35.5° and 38.7°, which referred to (002) and (111), showed that the CuO NP had a monoclinic structure, according to JCPDS card no.45-0937. The observed intense and sharp peaks showed good crystallinity of the prepared powder (El Sayed et al. 2015).

Fig.2. XRD pattern of synthesized CuO NPs

To clarify the particle size and surface morphology of the synthesized CuO particles, TEM and SEM images were examined. **Fig. 3** shows the TEM and SEM images of the CuO NPs. **Fig. 3a** reveals that the nanostructure homogeneity of CuO NPs resembled that obtained from the TEM image (Shammout et al. 2021, El Sayed et al. 2015). The TEM image shows that the CuO NPs were spherical. The TEM micrograph also showed that the nanospheres had an average diameter of about 7–18 nm. However, **Fig. 3b** shows that the nanostructure of CuO NPs resembled that obtained from the SEM image (Sharma et al. 2021). **Fig. 3b** shows the morphology of CuO NPs, exhibiting an almost spherical shape in arrangement.

Fig. 3. (a) TEM, (**b**) SEM images of synthesized CuO NPs

To examine its composition, the CuO NP was analyzed using EDX. This analysis was performed using the prepared sample to determine the Cu and O ratios **(Fig. 4a)**. The figure shows that only Cu and O elements were present in the prepared sample, thereby indicating the high purity of CuO in the sample. The appearance of sharp diffraction peaks **(Fig. 4a)** indicated the good crystallinity of the prepared NPs. The stoichiometric percentages of Cu and O were 55.94%, and 44.06%, respectively. The elemental mapping images of the prepared CuO NPs are shown in **Fig. 4b**. The images showed that the synthesized NPs contained Cu and O atoms, which agreed with the EDX analysis results. Furthermore, the elemental

mapping images showed united element dispersion and significant purity, and no meddlesome elements were observed.

Fig. 4. (a) EDX analysis and (b) mapping images of CuO NPs

Measurements of modified cotton fabric NPs

Mechanism of CMC–PEG–EG/Ag hydrogel loaded with CuO NPs

Fig. 5 shows a schematic diagram of CMC–PEG–EG/Ag when incorporated with different concentrations of CuO nanofiller. CMC and PEG hydrogel were formed using EG as a crosslinking agent, with stirring and heating, coated on the cotton fabric surface, and subsequently cured by EB radiation. The OH groups in PEG induced intermolecular and intramolecular hydrogen bonding. As CMC comprises multiple carboxyl groups, chemical crosslinking occurred between PEG and CMC in the presence of an EG monomer via stirring and heating and then EB radiation.

Fig.5. Schematic diagram of the compatibilizing mechanism of Ag/CuO NPs within the CMC/PEG hydrogel using EG as monomer on cotton fabrics surface

FTIR spectroscopy analysis

To explain the chemical reaction that occurred in the matrix utilized FTIR analysis which represented the effect of CuO reinforced the CMC–PEG–EG/Ag. **Fig. 6** illustrates the FTIR spectrum of the cotton fabrics (control), the unmodified cotton fabric surface by CMC–PEG–EG, and the modified cotton fabric using CMC–PEG–EG/Ag loaded by different contents of CuO. The FTIR spectra showed the characteristic peaks of the cotton fabrics (control) at 3422, 2896, and1160 cm^{-1}, corresponding to the –OH stretching vibrations, CH aliphatic stretching, and C–O stretching vibrations, respectively, whereas C–O–C asymmetric bridge stretching was attributed to 1032 cm^{-1} of the main peaks of the cellulose molecular structure. The peak at 1635 cm^{-1} was observed for O–H bending vibrations of the cellulose molecular. The IR spectra of CMC–PEG–EG on the cotton fabric surface showed the function groups attached to CMC, EG, and PEG polymers. The spectra of CMC–PEG–EG hydrogel exhibited a major peak at 3276 cm^{-1} due to intermolecular hydrogen bond (Liang and Marchessault, 1959); 2888 cm^{-1} was assigned to a hydrocarbon groupCH_2 stretching and 1712 cm^{-1} to a carbonyl group C=O stretching. An antisymmetrical vibration of the ionized carboxyl group COO–appeared at the band 1594 cm^{-1}(Petropavlovskii et al., 1984), the peak of the scissoring bending vibration of CH_2 was observed at 1419 cm^{-1}, and the bending vibration of CH was noticed at 1323 cm^{-1}(Hiroyuki 2014). The band limited to 1021 cm^{-1} was assigned to C–O of the stretching vibration of the cellulose fundamental (Adebajo and Frost 2004), whereas the band associated with 1249 cm^{-1} was attributed to C–O (alcohol). Therefore, the results suggested that CMC–PEG–EG existed on the cotton fabric surface, which resulted in the interpenetrating polymer network formation of CMC–PEG–EG on the cotton fabric. After incorporating different CuO NP contents with CMC/PEG/EG/Ag, the high or low intensity peaks were observed in the

FTIR spectra of the nanocomposite due to the peak position change. The same band appear at almost 554 cm^{-1} of CMC–PEG–EG/Ag (0.12%) and 0.5% CuO NPs, whereas the peak at 496 cm^{-1} was assigned to the CMC–PEG–EG/Ag/ 2 % CuO NPs. The intensity change and peak position revealed that the CuO NPs and CMC–PEG–EG/Ag matrix interacted (Shankar et al., 2017). Meanwhile, the peak appearing between 400 and 600 cm^{-1} may reflect the Cu–O mode (Chen et al., 2017).For loaded samples (CMC–PEG–EG/Ag) with different CuO NP contents, the absorption band appeared around 3330, 2897, 1712, 1606, 1420, 1327, 1248, and 1021 cm^{-1}, attributable to the –OH stretching, C–H stretching vibration, C=O stretching vibration, COO– antisymmetrical vibration, the scissoring bending vibration of CH_2, bending vibration of CH, C–O (alcohol), and C–O stretching vibration, respectively.

Fig. 6. Fourier transform infrared spectroscopy of unmodified cotton fabrics **(**pure**)** at 5 kGy**,** cotton fabrics by padding in CMC/PEG/EG at 5 kGy, cotton fabrics by padding in CMC/PEG/EG containing (0.006%) Ag/ (0.012%) CuO at 5 kGy, cotton fabrics by padding in CMC/PEG/EG containing (0.006%) Ag/ (0.5%) CuO at 25 kGy and (G) cotton fabrics by padding in CMC/PEG/EG containing (0.006%) Ag/ (2%) CuO at 5 kGy

Crosslinking density determination

The crosslinking density of polymer networks can be estimated from the stress–strain measurement (Eyssa et al., 2018). **Fig. 7** shows the impact of the CuO NP concentration and the radiation dose on the crosslinking density of the prepared CMC–PEG–EG/Ag nanocomposites. Observably, the crosslinking density increased as the CuO NP concentration increased to 0.5% and then declined when the CuO NP concentration reached 2%. The improvement in the crosslinking density at a CuO NP concentration of 0.5% confirmed the interfacial interactions between CMC–PEG–EG and CuO NPs (**Fig. 5**).The formation of hydrogen or coordinate bonds between the CMC–PEG–EG and CuO NPs created a strong structure, thereby increasing the crosslinking density in the CMC–PEG–EG/Ag (Hasheminya et al., 2018). In addition, a further increase in the CuO loading may result in excessive aggregation of CuO NPs, obstructing the occurrence of more crosslinking reactions within the CMC–PEG–EG. This may also cause a reduction in the physicomechanical characteristics of CMC–PEG–EG reinforced with CuO NPs (Mensaha et al., 2019). Moreover, **Fig. 7** shows the EB irradiation effects on the crosslinking density within the CMC–PEG–EG and its nanocomposites formulated by varying the CuO NP concentrations. Irradiation led to an appreciable increase in crosslinking density. The crosslinking density increased under a radiation dose until 25 kGy compared with the values obtained without EB radiation, confirming the formation of a progressive radiation-induced network.

Fig. 7. Variation of the crosslinking density of cotton fabrics by padding in CMC/PEG/EG, and cotton fabrics by padding in CMC/PEG/EG containing (0.006%) Ag/ different ratios of CuO NPs at various EB radiation doses

Morphology analysis by SEM

Fig. 8 shows the SEM cross-sectional morphologies of CMC–PEG–EG/Ag hydrogel modified cotton fabric containing various concentrations of CuO NPs (0.012%, 0.5%, 1%, and 2%) under irradiation doses (5 and 25 kGy). According to the data obtained from antibacterial studies, we selected samples that had superior properties over the others. As shown in **Fig. 8a**, the image shows smooth and homogeneous structures with a regular distribution of 0.012% CuO NPs on the cotton fabric surface. When we compared Graph (b) with Graph (a) in **Fig. 8**, the CuO NP concentration at 0.5% demonstrated a better uniform and homogeneous structure with regular distribution on the cotton fabric surface, necessitated by a stable polymeric blend network in addition to the strong interaction between the CuO particles and CMC–PEG–EG/Ag chains. The carboxylic acid groups ($-CO_2$) in CMC formed a coordinate bond with Cu ions (Ibarra et al., 2009) and were linked covalently to cotton via an esterification reaction with the cellulose hydroxyl groups when heated and EB irradiated. By increasing CuO NP concentration from 1% to 2%, some aggregations comprising CuO small particles on the cotton fabric were observed **(Fig. c and d)**. This means a stronger particle–particle interaction than the CuO–CMC–PEG–EG/Ag.

Fig. 8. Scanning electron micrographs of modified cotton fabrics by CMC/PEG/EG with Ag/ different ratios CuO NPs: (a) irradiated CMC/PEG/EG/ (0.006%) Ag/ (0.012%) CuO, (b) irradiated CMC/PEG/EG/ (0.006%) Ag/ (0.5%) CuO, (c) irradiated CMC/PEG/EG/ (0.006%) Ag/ (1%) CuO and (d) irradiated CMC/PEG/EG/ (0.006%) Ag/ (2%) CuO

Tensile mechanical properties

In most applications, mechanical properties are considered the most important physical properties of polymers. The stress–strain diagram is widely used to study mechanical parameters. **Figs. 9** and **10** show the influence of irradiation doses and different concentrations of CuO NPs on the tensile strength (TS) and elongation at break (%) of cotton fabrics padded with nanocomposite compounds containing CMC–PEG–EG/Ag/CuO hydrogels.

Herein, TS depended largely on the irradiation dose. The TSs of the unmodified and modified cotton fabrics both gradually increased when the irradiation dose was increased until a dose of 25 kGy. The increase in TS values until 25 kGy may be attributed to the presence of crosslinking density of compounds on the cotton surface. The enhancement in the stress values of the unirradiated and irradiated samples at 25 kGy of the cotton fabric nanocomposite formulations were 67% and 90%, respectively. However, the TS values increased by the incorporation of CuO NPs until 0.5% for the unirradiated and irradiated cotton fabrics covered with the CMC–PEG–EG/Ag/CuO hydrogel. The increase in the TS value could be due to the homogeneous distribution of CuO NPs in the CMC–PEG–EG polymer blend, which improved the interfacial interaction and load transfer between the CMC–PEG–EG and CuO NPs. This may also be due to the presence of the CuO NP ratio in the structure of the network that interrupts the H-bonding reactions between the COOH and OH groups of molecules and allows for the possible formation of adhesion (coordinate bonds) between CMC–PEG–EG polymer blend and copper ions [Ibarra et al., 2009], thereby leading to an increase in the TS of CMC–PEG–EG/Ag/CuO nanocomposites. However, the decreased TS values for the higher CuO NP concentration (1% and 2%)

were attributed to CuO NP–CuO NP particle agglomeration, leading to a poor interfacial reaction with CMC–PEG–EG. The high reactivity of nanoparticles leads to a large susceptibility to forming agglomerates, which could impede their advantages. Meanwhile, the TS of the modified cotton fabrics with the various compounds exceeded that of the unmodified fabric. This is due to the covering of fabrics with a thin layer of compounds, which resists tension. In addition, similar trends can be observed with elongation at break. The dispersion and density of inter and intramolecular interactions between the chains of polymer play important roles in the mechanical characteristics of polymer blends on cotton fabrics (Chambi, & Grosso, 2006).

Fig. 9. Variation of the tensile strength of cotton fabrics by padding in CMC/PEG/EG, and cotton fabrics by padding in CMC/PEG/EG containing (0.006%) Ag/ different ratios of CuO NPs at various EB radiation doses

Fig. 10. Variation of the elongation at break of cotton fabrics by padding in CMC/PEG/EG, and cotton fabrics by padding in CMC/PEG/EG containing (0.006%) Ag/ different ratios of CuO NPs at various EB radiation doses

WVP of modified cotton fabrics

WVP is proportionality persistent and is presumed to remain liberated of the water vapor grade practical crossways the films. However, hydrophilic substances, such as proteins and polysaccharide-based films, differ from this perfect performance owing to the contact of penetrating water molecules with polar groups of film components (Al-Muhtaseb et al., 2002). WVP is a significant parameter to be studied. Initially, the pervading particles abbreviate on superficial and solubilize addicted to the film. This is shadowed by dispersion in which infusing particles have to bargain their manner through the film. Lastly, these particles leave of absence the superficial of the film at other side. Modified cotton fabrics do not completely differ from unmodified cotton textiles. The obstruction of the holes with a slight modification marks the transport of vapor (Zeng et al., 2017). However, after the modification of the cotton fabrics with CMC–PEG–EG/Ag nanocomposites and different concentrations of CuO at a constant dose (5 kGy), the water vapor resistance were completely different. **Table 1** shows that the WVP of the unmodified textiles markedly exceeded that of the modified fabrics. In this case, the modification had a clear obstructive influence on the superficial of modified fabrics; thus, moisture transfer through the pores was prevented and the water vapor resistance of the modified fabrics was therefore higher. This is attributed to the CuO NPs that have low WVP (El Sayed et al. 2015, Shankar et al., 2017). The observed lower WVP values for modified cotton fabrics might be attributable to the hydrophobic nature of the CuO NPs. In addition, there is a possibility of H-bonding or coordinating link interactions between CuO NPs and OH groups existing in polymer chains inside the fabrics. These hydrogen bonding or coordinate bond connections might produce extra crosslinking inside the matrix system and therefore depress the dispersion of water vapors through films.

Thermal stability

The TGA thermograms and the corresponding rate of thermal decomposition reaction curves of unmodified cotton fabrics, the modified cotton fabrics with padding in CMC–PEG–EG and those padded with CMC–PEG–EG/Ag by loading in different CuO NP ratios and cured by EB radiation to a dose of 5 and 25 kGy are

illustrated in **Fig. 11**. The TGA thermograms showed a major decomposition stage within the temperature range 270°C–325°C for all fabrics. Furthermore, it can be noted that the thermal stability of all fabrics, either before or after padding, was roughly stable up to ~270°C. Yet, the modified cotton fabrics with the CMC–PEG–EG and CMC–PEG–EG/Ag using CuO NP ratios (0.12%, 0.5%, and 2%) demonstrated relatively higher thermal stability than the unmodified cotton fabrics. The corresponding rate of thermal decomposition reaction curves showed similar trends; yet, the temperatures of the maximum rate of reaction (T_{max}) of thermal decomposition vary from one material to another (**Fig. 11 and Table 2**). According to the values shown in **Fig. 11 and Table 2**, a few conclusions may be drawn:

- The unmodified cotton fabrics, modified cotton fabrics with padding in CMC–PEG–EG and those padded with CMC–PEG–EG/Ag by loading in different CuO NP ratios and cured by EB radiation appeared thermal decomposition through two T_{max} of the rate of thermal decomposition reaction because of the existence of multi-components in the hybrid fabric structures (Saleh et al. 2021).

- Generally, the modified cotton fabrics with CMC–PEG–EG and those with CMC–PEG–EG/Ag/different CuO NP ratios showed marked improvements in thermal stability with higher T_{max} values than the unmodified cotton fabrics. This could be attributed to the presence of chemical crosslinking reactions occurring between cotton cellulose and CMC–PEG–EG/Ag/CuO NP using EB irradiation (Shin et al.,2020). The highest enhancement in the thermal stability, for both the first and second T_{max}, was estimated in the case of modified cotton fabrics with CMC–PEG–EG/Ag/different CuO NP ratios. The results revealed that the thermal stability of the nanocomposites on cotton fabric surfaces increased by adding CuO NPs. This may be attributed to the ionic structure formation of Cu (Shankar et al., 2017).

Fig. 11. Thermogravimetric analysis and the corresponding rate of thermal decomposition of unmodified cotton fabrics **(**pure**)** at 5 kGy**,** cotton fabrics by padding in CMC/PEG/EG at 5 kGy, cotton fabrics by padding in CMC/PEG/EG containing (0.006%) Ag/ (0.012%) CuO at 5 kGy, cotton fabrics by padding in CMC/PEG/EG containing (0.006%) Ag/ (0.5%) CuO at 25 kGy and (G) cotton fabrics by padding in CMC/PEG/EG containing (0.006%) Ag/ (2%) CuO at 5 kGy

Antimicrobial activity of modified cotton fabrics

Evaluation by bacterial culture test

Microorganism growth on fabrics that touch the human body could cause some major problems, including producing distasteful scents, changing the color, and increasing the health hazard of utilizing such clothes. Some metal NPs, such as gold, silver, copper, and zinc, have been characterized as antimicrobial materials for applications. However, there is no accurate mechanism

to expound how metal NPs act and exterminate the bacteria. A probable mechanism is mentioned in the literature considering the formation of pits (Manikandan, M. Sathiyabama2017). It was suggested that the metal NPs initially adhere to the cell wall and then destroy the membrane of the bacteria cell wall, which causes the formation of pits. Thereafter, the pits formed prohibit the growth of the bacteria. The antimicrobial properties of cotton fabrics unmodified and modified with CMC/PEG/EG/Ag loaded in different CuO NP concentrations and EB irradiated at the different doses were examined against gram-positive bacteria (*Staphylococcus epidermis*) and gram-negative bacteria *(Escherichia coli*).

The antimicrobial properties were estimated in terms of inhibition zone (mm) (**Figs. 12, 13and 14**) and according to these figures and the value in Table 3, some points can be noticed:

(1) For the unmodified cotton samples (CMC/PEG/EG), not inhibition zones were observed against the growth of the two bacteria at all doses compared to 5 kGy, it found a small inhibition zone. This reveals that the unmodified fabrics have no antimicrobial ability.

(2) Generally, it can be observed clearly that fabrics modified with CMC/PEG/EG by adding Ag/CuO NPs displayed antimicrobial efficiency against the growth (S. *epidermis's*) and *(*E. *coli*) bacteria for all doses.

(3) By incorporating CuO NP concentration until 0.5%, modified fabrics demonstrated higher antimicrobial properties against the growth of (S. *epidermis's*) and *(*E. *coli*) bacteria at all doses compared with unmodified cotton samples. Meanwhile, when embedding 0.012% and 0.5% CuO NPs in modified cotton

fabrics showed higher antimicrobial properties at doses 5 and 25 kGy, respectively; the inhibition zones were 15 and 20 mm for (S. *epidermis's*) and *(*E. *coli*) bacteria, respectively (at 0.012% and 0.5% CuO NPs).

(4) Yet, the inhibition region was noticed that low slightly with the increment in CuO ratio (1%), when

increasing CuO concentration (2%) can see that the inhibition region increases again at the radiation dose 5 kGy, had 20 mm for (S. *epidermis's*) and 15 mm for *(*E. *coli*) bacteria.

(5) The dose 5 kGy exhibited higher antimicrobial property against the growth of (S. *epidermis's*) and *(*E. *coli*) bacteria for unmodified (CMC/PEG/EG) and modified cotton samples by adding Ag/CuO NPs at different concentrations (0.012%, 1%, and 2%), while the dose 25 kGy had higher antimicrobial properties for 0.5% CuO NPs.

The antimicrobial properties of cotton fabrics modified with Ag/CuO different ratios-based nanocomposites against (S. *epidermis's*) and *(*E. *coli*) could be explained as follows:

This behavior of the metal-nano-polymer composite is connected by a synergistic effect between Ag and CuO NPs in the polymer matrix that inclines the antibacterial efficiency of the nanocomposite compared to the alone nanoparticles, as justified by(Bogdanovic et al., 2015).At a low dose of electron beam 5kGy

was showed the highly reactivity against both *(*E. *coli*) and *(S. epidermis's)* bacteria which is probably as result of the polymers efficiency for long-term liberation, thus protracting the antibacterial action of nanocomposite(Cioffi et al., 2005) and the increment impact of the surface area related to the distribution of CuO and Ag NPs into the polymer.

Fig. 12. The antibacterial activities of the unmodified and modified cotton fabrics by CMC/PEG/EG with Ag/ different ratios CuO NPs: for code samples (1, 2, 3 and 4) of the unmodified cotton fabrics / CMC/PEG/EG, (5, 6, 7 and 8) of the modified cotton fabrics by CMC/PEG/EG/ (0.006%) Ag/ (0.012%) CuO, (9, 10, 11 and 12) of the modified cotton fabrics by CMC/PEG/EG/ (0.006%) Ag/ (0.5%) CuO, (13, 14, 15 and 16) of the modified cotton fabrics by CMC/PEG/EG/ (0.006%) Ag/ (1%) CuO, and (17, 18, 19 and 20) of the modified cotton fabrics by CMC/PEG/EG/ (0.006%) Ag/ (2%) CuO at various EB radiation doses against Gram +ve Bacteria

Fig. 13. The antibacterial activities of the unmodified and modified cotton fabrics by CMC/PEG/EG with Ag/ different ratios CuO NPs: for code samples (1, 2, 3 and 4) of the unmodified cotton fabrics / CMC/PEG/EG, (5, 6, 7 and 8) of the modified cotton fabrics by CMC/PEG/EG/ (0.006%) Ag/ (0.012%) CuO, (9, 10, 11 and 12) of the modified cotton fabrics by CMC/PEG/EG/ (0.006%) Ag/ (0.5%) CuO, (13, 14, 15 and 16) of the modified cotton fabrics by CMC/PEG/EG/ (0.006%) Ag/ (1%) CuO, and (17, 18, 19 and 20) of the modified cotton fabrics by CMC/PEG/EG/ (0.006%) Ag/ (2%) CuO at various EB radiation doses against Gram -ve Bacteria

Fig. 14. SEM images and dishes of cotton fabrics unmodified and modified against bacteria: (A) pure cotton fabrics without bacteria, (B) cotton fabrics by padding in CMC/PEG/EG at 0 kGy, (C) cotton fabrics by padding in CMC/PEG/EG at 5 kGy, (D) cotton fabrics by padding in CMC/PEG/EG at 25 kGy, (E) cotton fabrics by padding in CMC/PEG/EG containing (0.006%) Ag/ (0.012%) CuO at 5 kGy, (F) cotton fabrics by padding in CMC/PEG/EG containing (0.006%) Ag/ (0.5%) CuO at 25 kGy and (G) cotton fabrics by padding in CMC/PEG/EG containing (0.006%) Ag/ (2%) CuO at 5 kGy

Conclusions

Antibacterial fabrics, especially natural fabrics for biomedical applications, have large impacts on hygiene, exudates, and odor control and protection versus microbial attack. Small-sized CuO NPs were synthesized. The synthesized NPs were investigated by SEM, EDX, mapping image, TEM, and XRD analyses. Cotton fabrics were modified with polymer blends depending on CMC and PEG in the presence of EG loaded with Ag/CuO of different ratios of NPs. The modified cotton fabrics displayed high resistance for (E. *coli*) and *(S. epidermis)* bacteria at all CuO ratios (0.012%, 0.5%, and 2%). A remarkable improvement was also observed in the mechanical properties of cotton fabric after MC-PEG-EG/Ag/ratios CuO nanocomposite treatment until 0.5% CuO NPs and 25 kGy. The modified fabrics with CMC–PEG–EG/Ag/ratios CuO nanocomposite demonstrated superior antibacterial performance of (E. *coli*) and *(S. epidermis)* microorganisms. We concluded that the modified cotton fabrics with CMC–PEG–

EG/Ag/0.012% CuO nanocomposite and 5 kGy may be utilized as the modified best, due to the decrease in the cost of modifying the fabrics. It should be considered a potential candidate for medical purposes.

Declarations

Authors' contributions

H. M. Eyssa: Conceptualization, preparation the CuO nanoparticles, Software, Methodology, Formal analysis, Investigation, data curation, Visualization, Original draft preparation - Reviewing and Editing. **R. M. Attia**: Data curation, Formal analysis, Visualization, Resources, Original draft preparation- Writing and Reviewing.**R.F. Sadeck**: Preparation microbiology section, Investigation, Resources. All authors read and approved the final manuscript.

Acknowledgements

We greatly appreciate the financial support of National Center for Radiation Research and Technology for help to perform the analyses of this work. Egyptian Atomic Energy Authority, Cairo, Egypt.

Ethics approval: This study does not involve human participants, animals, and potential conflicts of interest (The authors state that they have no known personal connections regarding any possible experiments performed on people or animals).

Consent to participate: Not applicable.

Consent for publication Not applicable.

Availability of data and materials Not applicable.

Competing interests: The authors declare they have no competing interests, and all authors have given their approval for publication. The authors state that the study reported was unique and had never been published before.

Funding No funding was received for conducting this study.

References

Abdollahi, M., Damirchi, S., Shafafi, M., Rezaei, M., & Ariaii, P. (2019) Carboxymethyl cellulose agar biocomposite film activated with summer savory essential oil as an antimicrobial agent, *International Journal of Biological Macromolecules*, *126,* 561–568, https://doi.org/10.1016/j.ijbiomac.2018.12.115.

Adebajo, M.O., & Frost, R.L. (2004). Acetylation of Raw Cotton for Oil Spill Cleanup Application - An FTIR and 13C MAS NMR Spectroscopic Investigation. *Spectrochimica Acta, Part A:* Molecular and *Biomolecular Spectroscopy, 60*(10), 2315-2321. https://doi.org/10.1016/j.saa.2003.12.005.

Al-Muhtaseb, A. H., Mcminn, W. A. M., Mage, T. R. A. (2002). Moisture Sorption Isotherm Characteristics of Food Products: A Review, *Food Bioproducts Process*, *80*, 118-128. https://doi.org/10.1205/09603080252938753.

Bogdanovic, U., Vodnik, V., Mitric, M., Dimitrijevic, S., Skapin, S. D. V., Budimir, Z. M., & M. Stoiljkovic (2015). Nanomaterial with High Antimicrobial Efficacy Copper/Polyaniline Nanocomposite. *ACS applied materials & interfaces*, 7(3), 1955-1966. DOI: 10.1021/am507746m.

Bozaci, E., Akar, E., Ozdogan, E., Demir, A., Altinisik, A., & Seki, Y.(2015). Application of carboxymethylcellulose hydrogel based silver nanocomposites on cotton fabrics for antibacterial property, *Carbohydrate Polymers* http://dx.doi.org/10.1016/j.carbpol.2015.07.036.

Capanema, N. S. V., Mansur, A. A. P., Jesus, A. C. D., Carvalho, S. M., Oliveira, L. C. D., & Mansur, H. S. (2018). Superabsorbent crosslinked carboxymethyl cellulose-PEG hydrogels for potential wound dressing applications, *International Journal of Biological Macromolecules*, *106*, 1218-1234. https://doi.org/10.1016/j.ijbiomac.2017.08.124

Chambi, H., & Grosso, C. (2006). Edible films produced with gelatin and casein cross-linked with transglutaminase. *Food Research International*, *39*, 458–466. https://doi.org/10.1016/j.foodres.2005.09.009

Chen, W., Chen, J., Feng, Y. B., Hong, L., Chen, Q.Y., Wu, L.F., Lin, X.H., & Xia, X.H. (2012).Peroxidase-like activity of water-soluble cupric oxide nanoparticles and its analytical application for detection of hydrogen peroxide and glucose. *Analyst*, *137*, 1706–1712. DOI: 10.1039/C2AN35072F.

Cioffi, N. L., Torsi, N., Ditaranto, G., Tantillo, L., Ghibelli, L., Sabbatini, T., Bleve-Zacheo, M. D'Alessio, P. G. Zambonin and E. Traversa (2005). Copper nanoparticle/polymer composites with antifungal and bacteriostatic properties. Chemistry of Materials 17(21): 5255-5262. https://doi.org/10.1021/cm0505244.

Dahlan, N. A., Teow, S. Y., Lim, Y. Y., Pushpamalar, J. (2021). Modulating carboxymethylcellulose-based hydrogels with superior mechanical and rheological properties for future biomedical applications, *expressPolymer Letters*, 15 (7), 612–625. https://doi.org/10.3144/expresspolymlett.2021.52.

Dastjerdi, R., & Montazer, M. (2010).A review on the application of inorganic nano-structured materials in the modification of textiles: Focus on anti-microbial properties. *Colloid. Surface. B*, *79*, 5-18. https://doi.org/10.1016/j.colsurfb.2010.03.029.

DeBoer, T.R., Chakraborty, I., & Mascharak, P.K. (2015). Design and construction of a silver (I)-loaded cellulose-based wound dressing: trackable and sustained release of silver for controlled therapeutic delivery to wound sites, *J. Mater. Sci. Mater. Med. 26*,243. https://doi.org/10.1007/s10856-015-5577-1.

Elmaaty, T. A., Okubayashi, S., Elsisi, H., & Abouelenin, S. (2022). Electron beam irradiation treatment of textiles materials: a review, *Journal of Polymer Research*, *29*, 117. https://doi.org/10.1007/s10965-022-02952-4.

El-Naggar, W. M., Zohdy, M. H., Said, H. M., El-Din, M. S., & Noval, D. M. (2005). Pigment colors printing on cotton fabrics by surface coating induced by electron beam and thermal curing, *Applied Surface Science*, *241*, 420–430. https://doi.org/10.1016/j.apsusc.2004.07.039

El Sayed, A. M., El-Gamal, S., Morsi, W. M., & Mohammed, Gh. (2015). Effect of PVA and copper oxide nanoparticles on the structural, optical, and electrical properties of carboxymethyl cellulose films, *J. Material Sci*ence, *50*, 4717–4728. DOI 10.1007/s10853-015-9023-z.

Eyssa, H.M., Abulyazied, D.E., & Abo-State, M. A. M. (2018). Application of Polyurethane/ Gamma Irradiated Carbon Nanotubes Composites as Antifouling Coat *J.Polymer Composite., 39***,** E1196-1206. DOI 10.1002/pc.24718.

Eyssa, H.M., Sawires, S.G., &Senna, M.M. (2019). Gamma Irradiation of Polyethylene Nanocomposites for Food Packaging Applications against Stored-Product Insect Pests. *J. Vinyl. Additive. Technology*, *25*, 120-129. DOI 10.1002/vnl.21660.

Eyssa, H.M., El Mogy, S. A., & Youssef, H. A. (2021). Impact of Foaming Agent and Nanoparticle Fillers on the Properties of Irradiated Rubber. *Radiochimica. Acta*, *109*(2), 127-142. https://doi.org/10.1515/ract-2020-0015

Hasheminya, M.S., Mokarram, R.R., Ghanbarzadeh, B., Hamishekar, H., Kafil, H. S., & Dehghannya, J. (2019).Influence of simultaneous application of copper oxide nanoparticles and *Satureja Khuzestanica* essential oil on properties of kefiran–carboxymethyl cellulose films, *Polymer Testing*, *73*, 377-388. https:// doi.org/10.1016/j.polymertesting12.002.

Hebeish, A.A., Abdelhady, M.M., Youssef, A.M. (2013). TiO_2 nanowire and TiO_2 nanowire doped Ag-PVP nanocomposite for antimicrobial and self-cleaning cotton textile, *Carbohydrate Polymers 91* (2013) 549–559. http://dx.doi.org/10.1016/j.carbpol.2012.08.068

Ibarra, L., Rodríguez A., Barrantes, I. M. (2009). Crosslinking of carboxylated nitrile rubber (XNBR) induced by coordination with anhydrous coppersulfate),*Polym.. Inter 58*, 218-226. https:// doi. org/10.1002/pi.2519.

Kanikireddy, V., Varaprasad, K., Jayaramudu, T., Karthikeyan, Ch., & R., Sadiku, (2020). Carboxymethyl cellulose-based materials for infection control and wound healing, *International Journal of Biological Macromolecules*, *164*, 963–975. https://doi.org/10.1016/j.ijbiomac.2020.07.160

Khafaga, M. R., Ali H. E., & El-Naggar, W. M. (2015). Antimicrobial finishing of cotton fabrics based on gamma irradiated carboxymethyl cellulose/poly(vinyl alcohol)/TiO2 nanocomposites, *The Journal of The*

Textile Institute, http://dx.doi.org/10.1080/00405000.2015.1061762

Kono, H. (2014). Characterization and properties of carboxymethyl cellulose hydrogels crosslinked by polyethylene glycol, *Carbohydrate Polymers*, *106*, 84–93. https://doi.org/10.1016/ j.carbpol. 2014.02020.

Lee, J.H., Nho, Y.C., Lim, Y.M., & Son, T.I. (2005). Prevention of Surgical Adhesions with Barriers of Carboxymethylcellulose and Poly (ethylene glycol) Hydrogels Synthesized by Irradiation, *J. Applied Polymer Science*, *96*, 1138–1145. https://doi.org/10.1002/app.21558.

Liang, C. Y., Marchessault, R.H. (1959). Infrared spectra of crystalline polysaccharides. II. Native celluloses in celluloses in the region from 640 to 1700 cm^{-1}. *J. Polymer Sci*ence, XXXIX, 269-278. https://doi.org/10.1002/ pol.1959.1203913521.

Lin, C.C., & Anseth, K.S. (2009). PEG hydrogels for the controlled release of biomolecules in regenerative medicine, *Pharm. Res*, *26* (3), 631–643. Doi: 10.1007/s11095-008-9801-2.

Lustosa, A., Oliveira, A. D. J., Quelemes, P., Plácido, A., Silva, F. D., Oliveira, I., M. Almeida, D., Amorim, A., Matos, C. D., Oliveira, R.D., Silva, D. D., Eaton, Leite, P. J. D. A. (2017). In situ synthesis of silver nanoparticles in a hydrogel of carboxymethyl cellulose with phthalated-cashewgumas a promising antibacterial and healing agent, *Int. J. Mol. Sci,18*, 2399. https://doi.org/10.3390/ ijms18112399.

Manikandan, A., & Sathiyabama, M. (2015). Green Synthesis of Copper-Chitosan Nanoparticles and Study of its Antibacterial Activity, *Nanomedicine & Nanotechnology 6*, 2–5. http://dx.doi.org/10.4172/2157-7439.1000251.

Mensaha, B., Guptab, K.C., Kanga, G. Leea, H., Nah, C. (2019). A comparative study on vulcanization behavior of acrylonitrile-butadiene rubber reinforced with graphene oxide and reduced graphene oxide as fillers, Polym. Test. 76, 127–137. https://doi.org/10.1016/j.polymertesting.2019.01.026.

Petropavlovskii, G. A., Larina, E.I., Borisova, T.I. (1984). *Cellulose Chem. Technol., 187*(3), 283-292.

Saleh N. S., Khaffaga, M. M., Ali, N. M., Hassan, M. S., El-Naggar, W. M., & Rabie, G. M. (2021). Anti-bacterial functionalization of cotton and cotton/polyester fabrics applying hybrid coating of copper/chitosan nanocomposites loaded polymer blends via gamma irradiation, *International Journal of Biological Macromolecules*, *183*, 23–34. https://doi.org/10.1016/j.ijbiomac.2021.04.059.

Sanad, M.H., Eyssa, H.M., Gomaa, N.M., Marzook, F.A., & Bassem, S.A. (2021). Radioiodinated esomeprazole as a model for peptic ulcer localization *Radiochimica Acta*, 109(9), 711–718. https: //doi.org/10.1515/ract-2021-1056.

Sanad, M. H., Eyssa, H. M., Marzook, F. A., Farag, A. B., Rizvi, S. F. A., Mandal, S. K., Patnaik, S. S., Fouzy, A. S. M., Sabry A. B. & Verpoort, F. (2021). Radiosynthesis and Biological Evaluation of ^{99m}Tc Nitrido-

Levetiracetam as a Brain Imaging Agent, *Radiochemistry*, *63*, 635–641. DOI: 10.1134/S106636222105012X.

Sanad, M. H., Eyssa, H. M., Marzook, F. A., Farag, A. B., Rizvi, S. F. A., Mandal, S. K., Patnaik, S. S., Fouzy, A. S. M., Sabry A. B. & Verpoort, F. (2021). Comparative Bioevaluation of ^{99m}Tc Tricarbonyl and ^{99m}Tc-Sn (II) Lansoprazole as a Model for Peptic Ulcer Localization, *Radiochemistry*, *63*, 642–650. DOI: 10.1134/S106636222105012X.

Selvarani, T., Prabhu B., & Thenmozhi, K. (2013). Effect of aqueous extract from the sea weed, Sargassum illicifolium, on three types of non-pathogenic terrestrial bacteria. *International Journal of Medicinal and Aromatic Plants*, *3*(2), 169-177.

Shammout, M. W., & Awwad, A. M. (2021). A novel route for the synthesis of copper oxide nanoparticles using *Bougainvillea* plant flowers extract and antifungal activity evaluation, *Chemistry International, 7*(1), 71-78. DOI:10.5281/zenodo.4042902.

Shankar, S., Wang, L.F. & Rhim, J.W. (2017). Preparation and properties of carbohydrate-based composite films incorporated with CuO nanoparticles, *Carbohydrate Polymers*, *169*, 264–271, https://doi.org/10.1016/ j.carbpol.2017.04.025.

Sharma, S., Kumar, K., Thakur, N., Chauhan, S., & Chauhan, M. S. (2021). Eco-friendly *Ocimum tenuiflorum* green route synthesis of CuO nanoparticles: Characterizations on photocatalytic and antibacterial activities, *Journal of Environmental Chemical Engineering*, *9*, 105395. https://doi.org/10.1016/j.jece.2021.105395.

Shahid, I., ul., Shahid, M., & Mohammad, F. (2013). Green Chemistry Approaches to Develop Antimicrobial Textiles Based on Sustainable Biopolymers—A Review. *Ind. Eng.Chem. Res., 52*, 5245- 5260. https://doi.org/10.1021/ie303627x.

Shin, J.Y., Lee, D. Y., Kim, B.Y., & Yoon, J. I. (2020). Effect of polyethylene glycol molecular weight on cell growth behavior of polyvinyl alcohol/carboxymethyl cellulose/polyethylene glycol hydrogel*, J Appl Polym Sci*, *137*,:e49568. https://doi.org/10.1002/app.49568.

Thite A.G., Krishnanand K., Sharma D.K., & Mukhopadhyay A.K. (2018). Multifunctional finishing of cotton fabric by electron beam radiation synthesized silver nanoparticles. Rad. Phys. Chem, *153*,173–179. https:// doi. org/10. 1016/j. radph yschem. 2018. 09. 023.

Wang, P., Zhang, M.Y., Qu, J.H., Wang, L.J., Geng, J.Z., Fu, F.Y., & Liu, X.D., (2022). Antibacterial cotton fabric prepared by a “grafting to” strategy using a QAC copolymer, *Cellulose*, *29*, 3569–3581. https://doi. org/10.1007/s10570-022-04469-x.

Xu, Q.B., Wu, Y.H., Zhang, Y.Y., Fu, F.Y., & Liu. X.D. (2016). Durable Antibacterial Cotton Modified by Silver Nanoparticles and Chitosan Derivative Binder, *Fibers and Polymers, 17,* (11), 1782-1789, DOI

10.1007/s12221-016-6609-2.

Zang, Y.H, Muller, R., & Froelich, D. (1989). Determination of crosslinking density of polymer networks by mechanical data in simple extension and by swelling degree at equilibrium. *J. Polymer, 30*, 2060-2062. https://doi.org/10.1016/0032-3861 (89)90294-2.

Zeng, Li, N., Wang, F., Hu, Y., Qu, D., Luan, W., Dong, Y., Zhang, S., J., & Bai, Y. (2017). Fluorinated polyurethane based on liquid fluorine elastomer (LFH) synthesis via two-step method: The critical value of thermal resistance and mechanical properties. *RSC Adv*, *7*, 30970–30978. DOIhttps://doi.org/10.1039/C7R A04509C.

Tables

Table 1. Water vapor permeability for unmodified and modified cotton fabrics with Ag/different ratios of CuO nanoparticles cured with EB radiation at 5 kGy.

Sample	Dose, kGy	Water vapor permeability %
Unmodified cotton fabrics	5	0.33
Modified cotton fabrics with CMC-PEG-EG	5	0.25
Modified cotton fabrics with CMC-PEG-EG/Ag 0.006% / CuO 0.012%	5	0.13
Modified cotton fabrics with CMC-PEG-EG/Ag 0.006% / CuO 0.5%	5	0.12
Modified cotton fabrics with CMC-PEG-EG/Ag 0.006% / CuO 1%	5	0.10
Modified cotton fabrics with CMC-PEG-EG/Ag 0.006% / CuO 2%	5	0.09

Table 2

Temperatures of the maximum rate of reaction T_{max} (°C) of thermal decomposition of pure cotton fabrics, unmodified cotton fabrics / CMC-PEG-EG**,** modified cotton fabrics with CMC-PEG-EG/Ag 0.006% / CuO 0.012%**,** modified cotton fabrics with CMC-PEG-EG/Ag 0.006% / CuO 0.5% and modified cotton fabrics with CMC-PEG-EG/Ag 0.006% / CuO 2%. The irradiation dose was at 5 and 25 kGy.

Samples	Dose, kGy	1st T_{max} (°C)	2nd T_{max} (°C)
Pure cotton fabrics	5	321	381
Unmodified cotton fabrics / CMC-PEG-EG	5	324	404
Modified cotton fabrics with CMC-PEG-EG/Ag 0.006% / CuO 0.012%	5	325	414
Modified cotton fabrics with CMC-PEG-EG/Ag 0.006% / CuO 0.5%	25	327	422
Modified cotton fabrics with CMC-PEG-EG/Ag 0.006% / CuO 2%	5	328	430

Table 3. Inhibition zone of unmodified and modified cotton fabrics with different concentration of CuO NPs for gram-positive and gram-negative with EB radiation.

Code sample	Conc of Ag/CuO %	Radiation dose, kGy	Inhibition zone(mm)	
			gram-positive	gram-negative
1	0/0	0	0	0
2	0/0	5	8	8
3	0/0	10	0	0
4	0/0	25	0	0
5	0.006/0.012	0	10	12
6	0.006/0.012	5	15	20
7	0.006/0.012	10	10	20
8	0.006/0.012	25	15	20
9	0.006/0.5	0	20	9
10	0.006/0.5	5	10	15
11	0.006/0.5	10	17	10
12	0.006/0.5	25	15	20
13	0.006/1	0	20	10.05
14	0.006/1	5	9	14
15	0.006/1	10	9	15
16	0.006/1	25	11	9
17	0.006/2	0	10	10
18	0.006/2	5	20	15
19	0.006/2	10	10	16
20	0.006/2	25	10	13

Figures

Figure 1

Schematic diagram for the preparation of CuO NPs

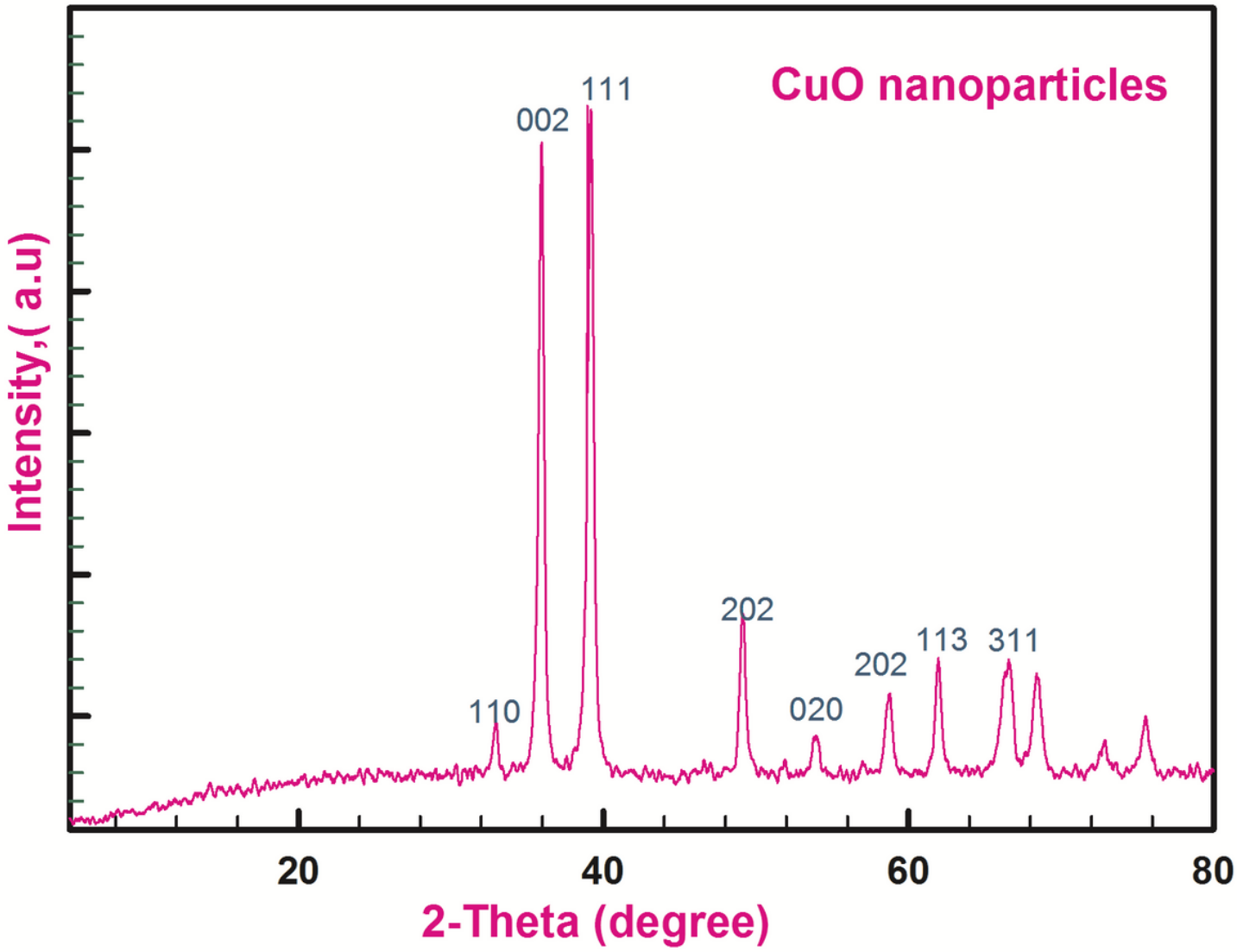

Figure 2

XRD pattern of synthesized CuO NPs

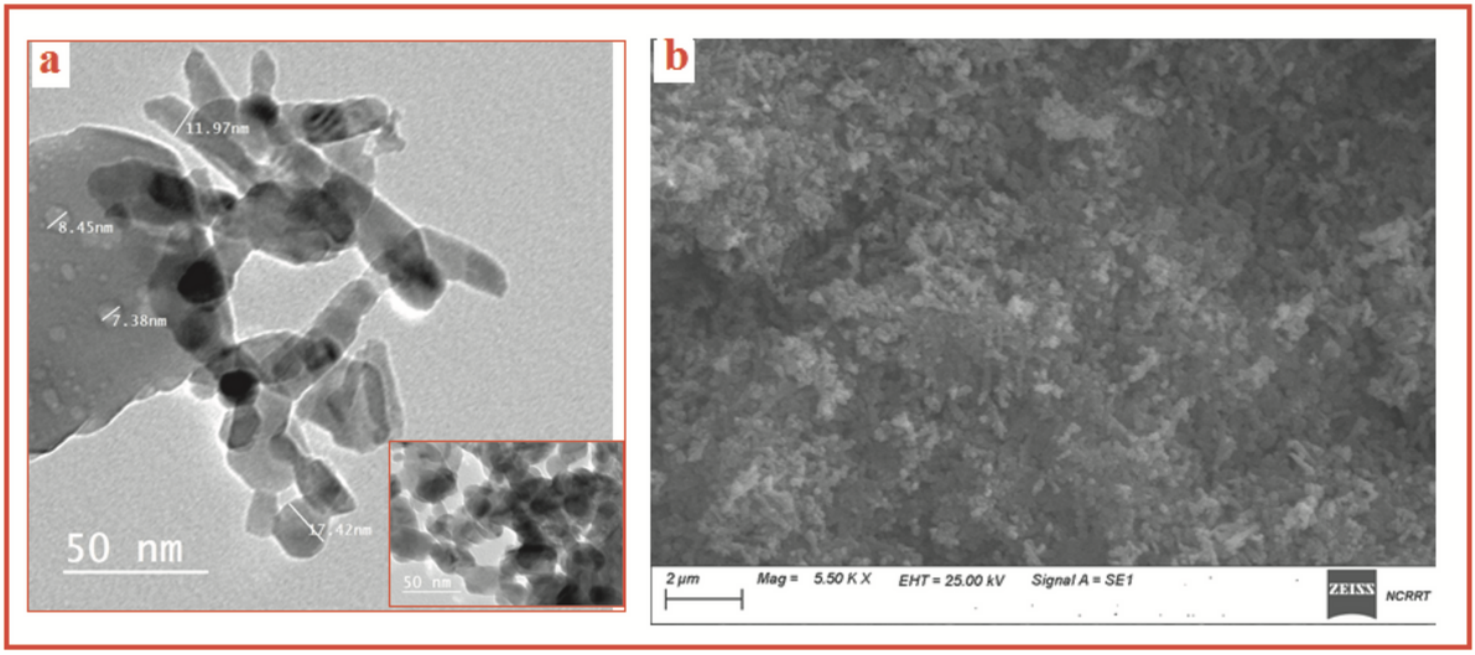

Figure 3

(a) TEM, (**b**) SEM images of synthesized CuO NPs

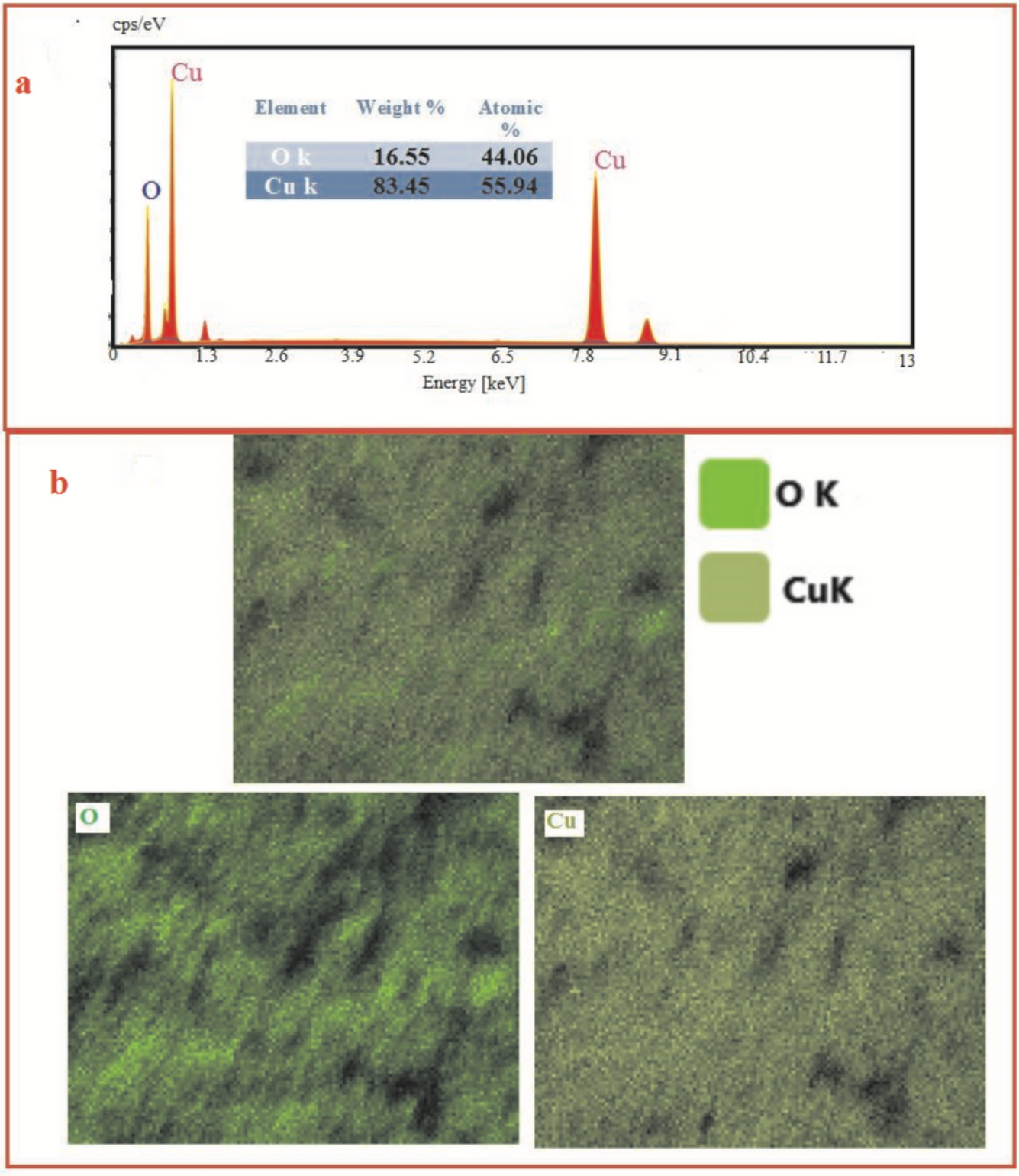

Figure 4

(a) EDX analysis and (b) mapping images of synthesized CuO NPs

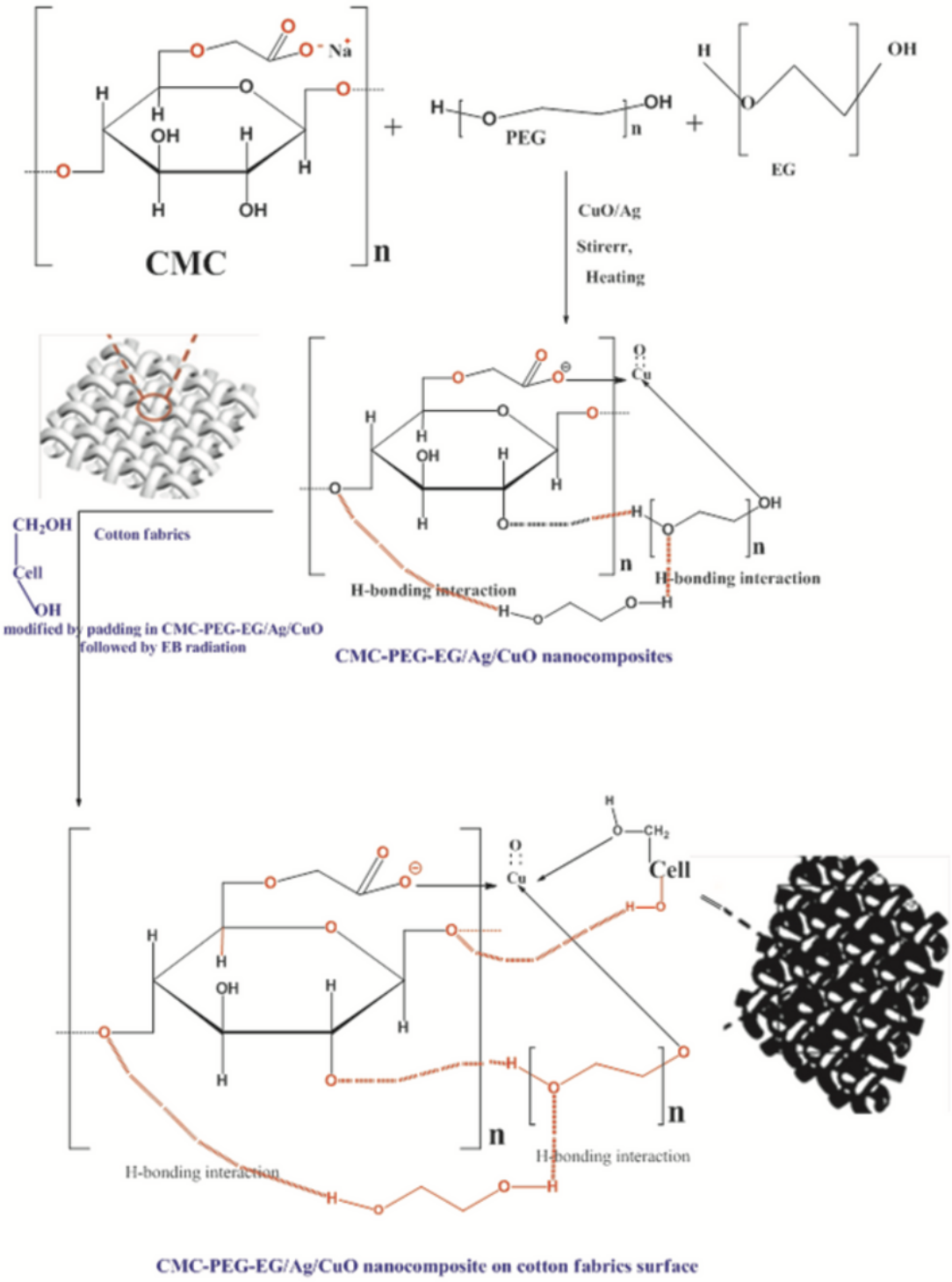

Figure 5

Schematic diagram of the compatibilizing mechanism of Ag/CuO NPs within the CMC/PEG hydrogel using EG as monomer on cotton fabrics surface

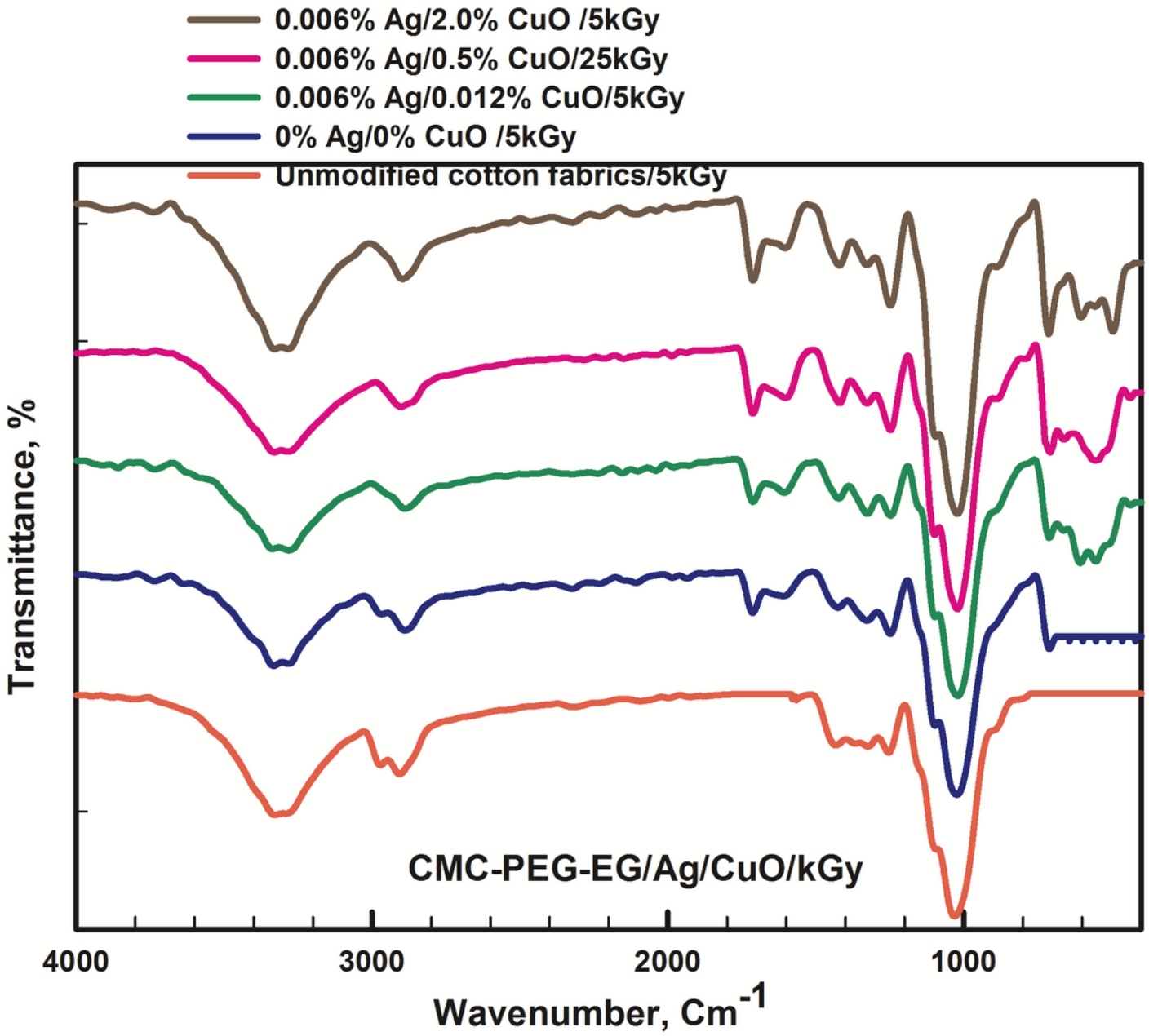

Figure 6

Fourier transform infrared spectroscopy of unmodified cotton fabrics (pure) at 5 kGy, cotton fabrics by padding in CMC/PEG/EG at 5 kGy, cotton fabrics by padding in CMC/PEG/EG containing (0.006%) Ag/ (0.012%) CuO at 5 kGy, cotton fabrics by padding in CMC/PEG/EG containing (0.006%) Ag/ (0.5%) CuO at 25 kGy and (G) cotton fabrics by padding in CMC/PEG/EG containing (0.006%) Ag/ (2%) CuO at 5 kGy

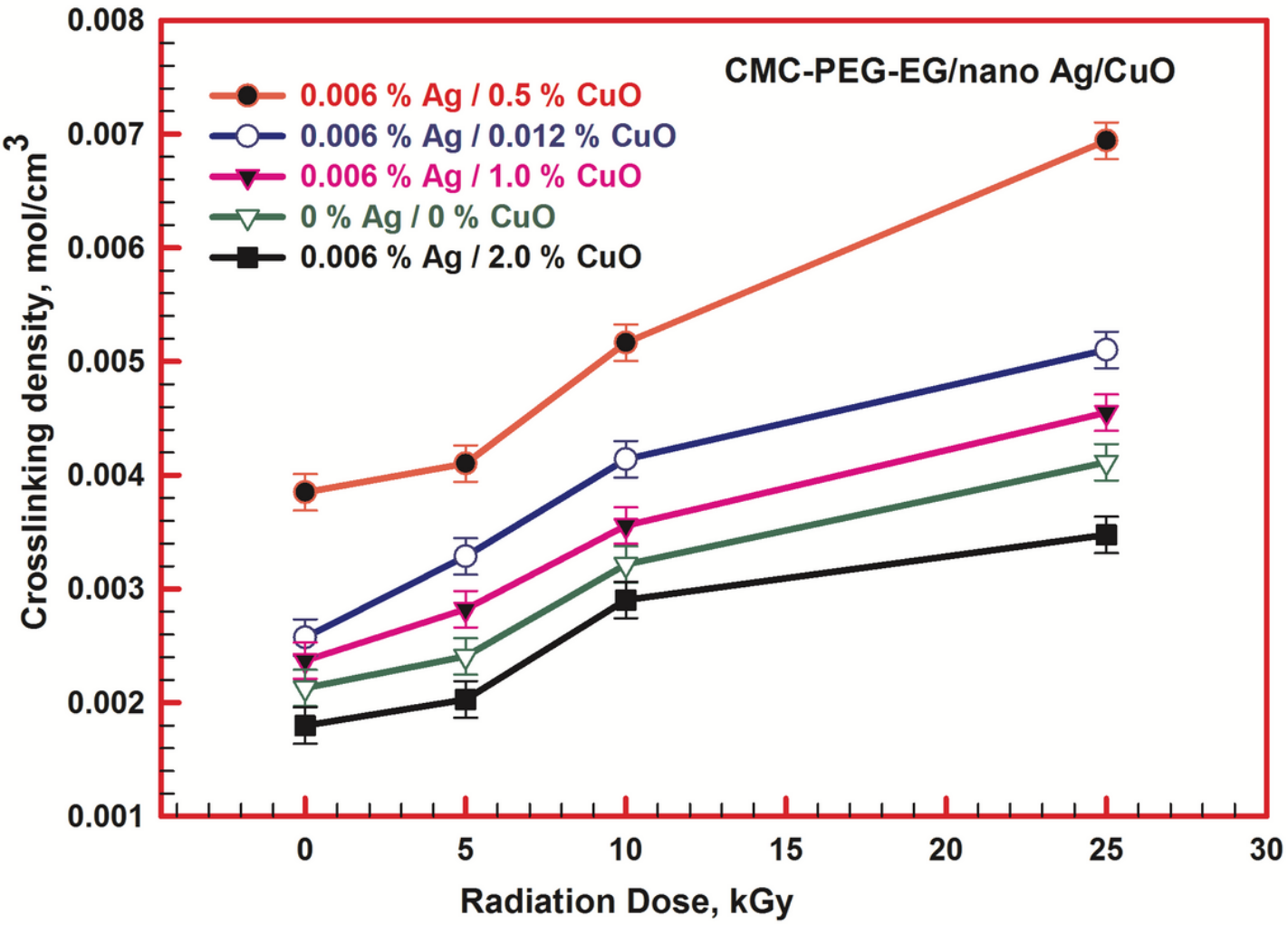

Figure 7

Variation of the crosslinking density of cotton fabrics by padding in CMC/PEG/EG, and cotton fabrics by padding in CMC/PEG/EG containing (0.006%) Ag/ different ratios of CuO NPs at various EB radiation doses

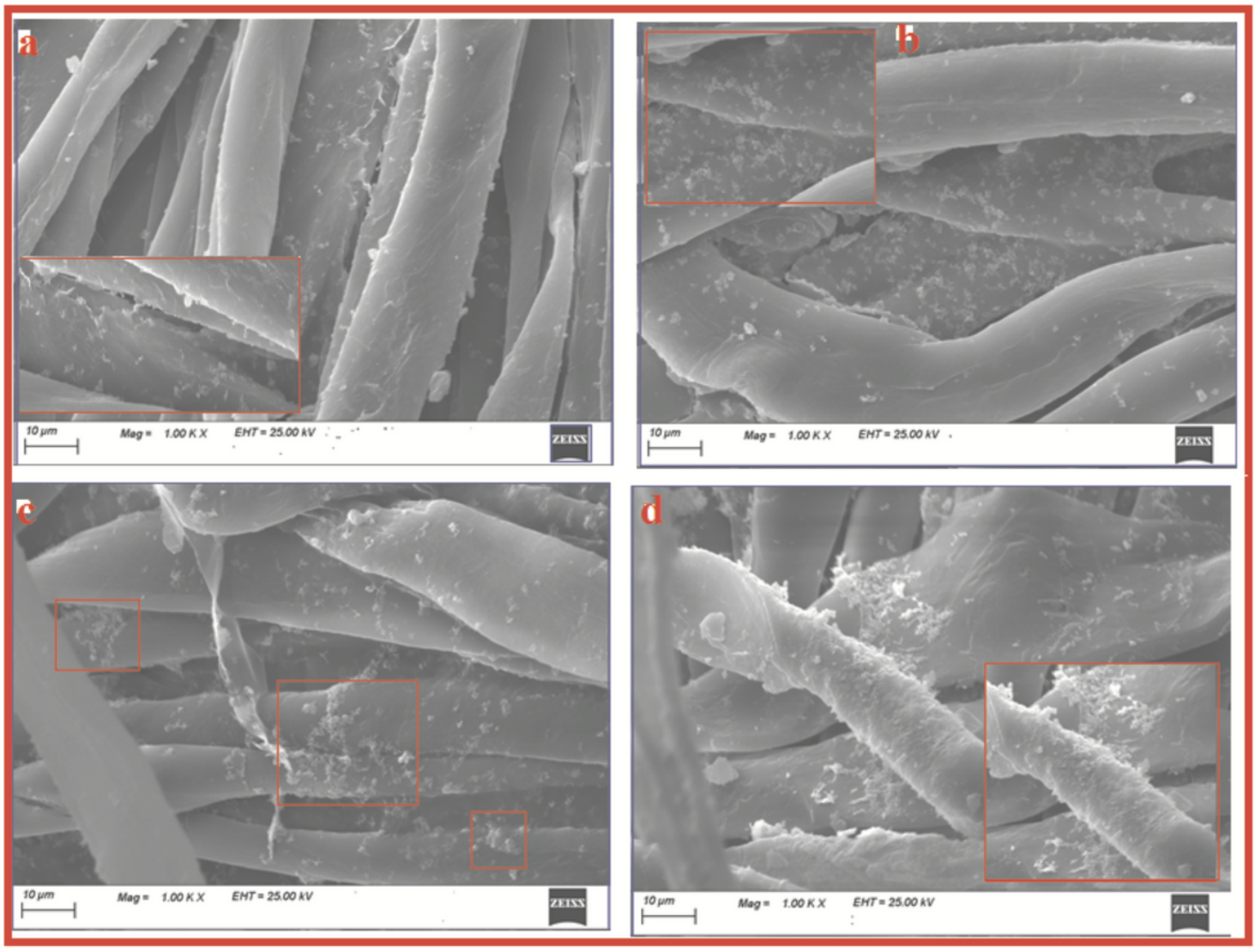

Figure 8

Scanning electron micrographs of modified cotton fabrics by CMC/PEG/EG with Ag/ different ratios CuO NPs: (a) irradiated CMC/PEG/EG/ (0.006%) Ag/ (0.012%) CuO, (b) irradiated CMC/PEG/EG/ (0.006%) Ag/ (0.5%) CuO, (c) irradiated CMC/PEG/EG/ (0.006%) Ag/ (1%) CuO and (d) irradiated CMC/PEG/EG/ (0.006%) Ag/ (2%) CuO

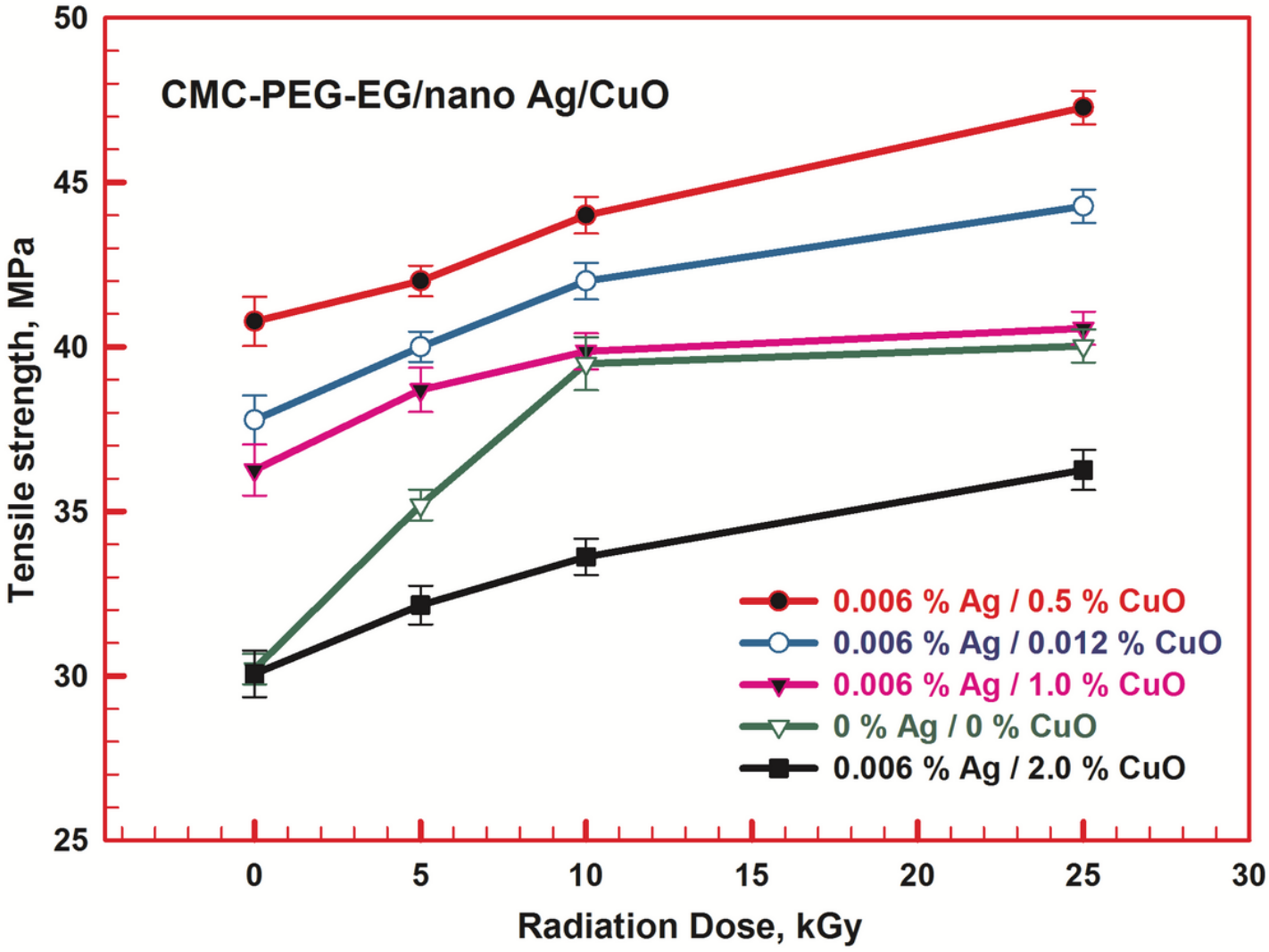

Figure 9

Variation of the tensile strength of cotton fabrics by padding in CMC/PEG/EG, and cotton fabrics by padding in CMC/PEG/EG containing (0.006%) Ag/ different ratios of CuO NPs at various EB radiation doses

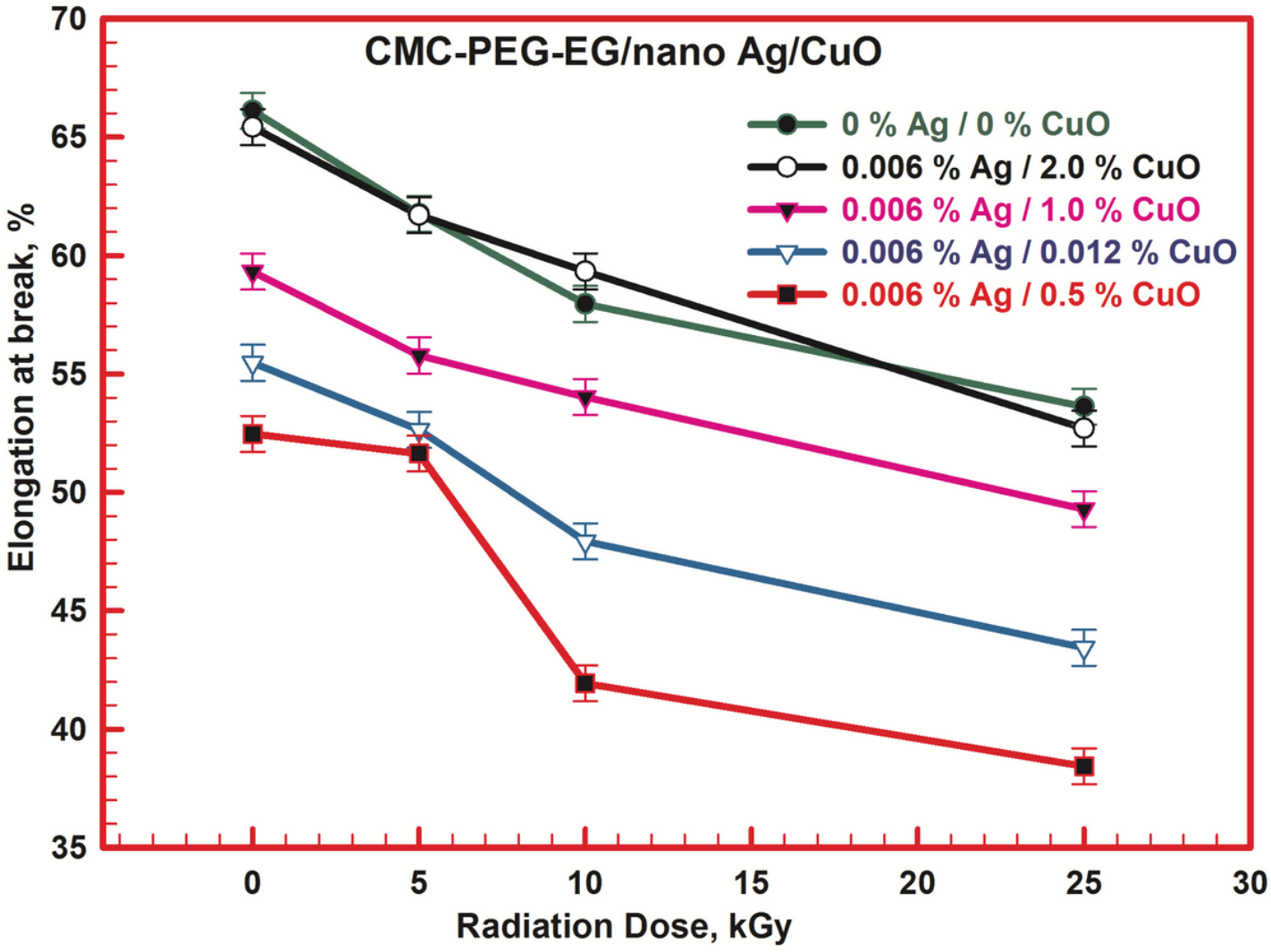

Figure 10

Variation of the elongation at break of cotton fabrics by padding in CMC/PEG/EG, and cotton fabrics by padding in CMC/PEG/EG containing (0.006%) Ag/ different ratios of CuO NPs at various EB radiation doses

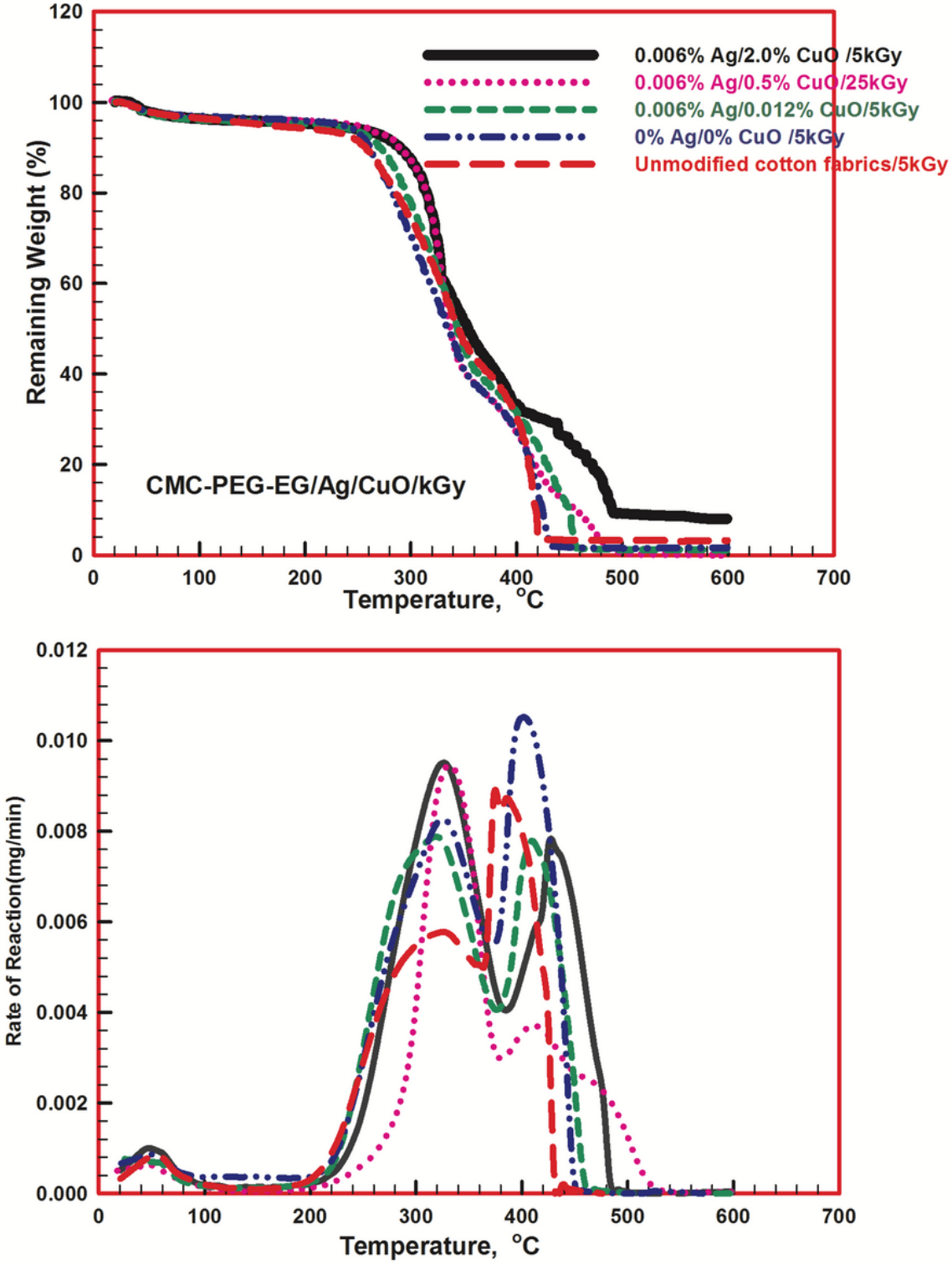

Figure 11

Thermogravimetric analysis and the corresponding rate of thermal decomposition of unmodified cotton fabrics (pure) at 5 kGy, cotton fabrics by padding in CMC/PEG/EG at 5 kGy, cotton fabrics by padding in CMC/PEG/EG containing (0.006%) Ag/ (0.012%) CuO at 5 kGy, cotton fabrics by padding in CMC/PEG/EG containing (0.006%) Ag/ (0.5%) CuO at 25 kGy and (G) cotton fabrics by padding in CMC/PEG/EG containing (0.006%) Ag/ (2%) CuO at 5 kGy

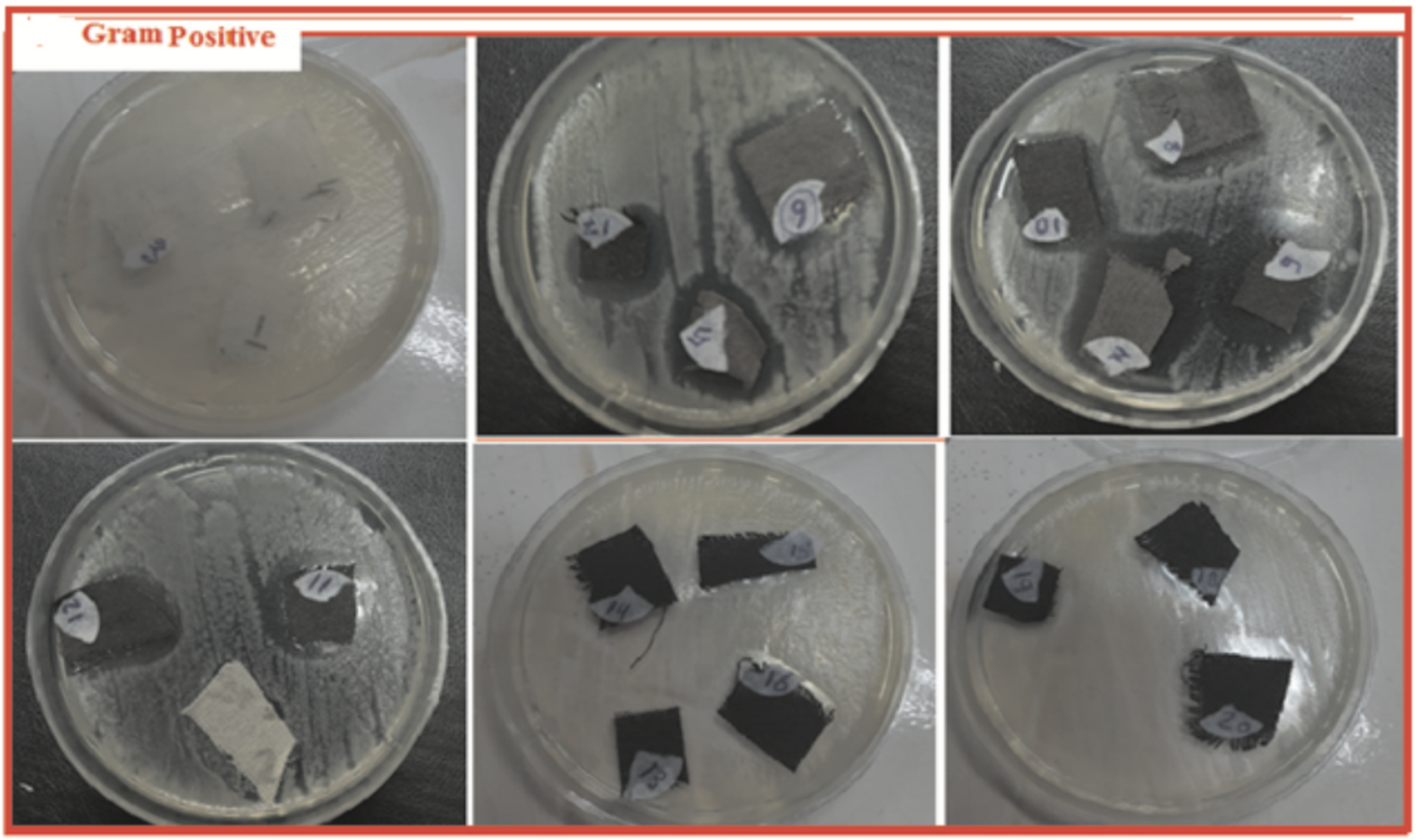

Figure 12

The antibacterial activities of the unmodified and modified cotton fabrics by CMC/PEG/EG with Ag/ different ratios CuO NPs: for code samples (1, 2, 3 and 4) of the unmodified cotton fabrics / CMC/PEG/EG, (5, 6, 7 and 8) of the modified cotton fabrics by CMC/PEG/EG/ (0.006%) Ag/ (0.012%) CuO, (9, 10, 11 and 12) of the modified cotton fabrics by CMC/PEG/EG/ (0.006%) Ag/ (0.5%) CuO, (13, 14, 15 and 16) of the modified cotton fabrics by CMC/PEG/EG/ (0.006%) Ag/ (1%) CuO, and (17, 18, 19 and 20) of the modified cotton fabrics by CMC/PEG/EG/ (0.006%) Ag/ (2%) CuO at various EB radiation doses against Gram +ve Bacteria

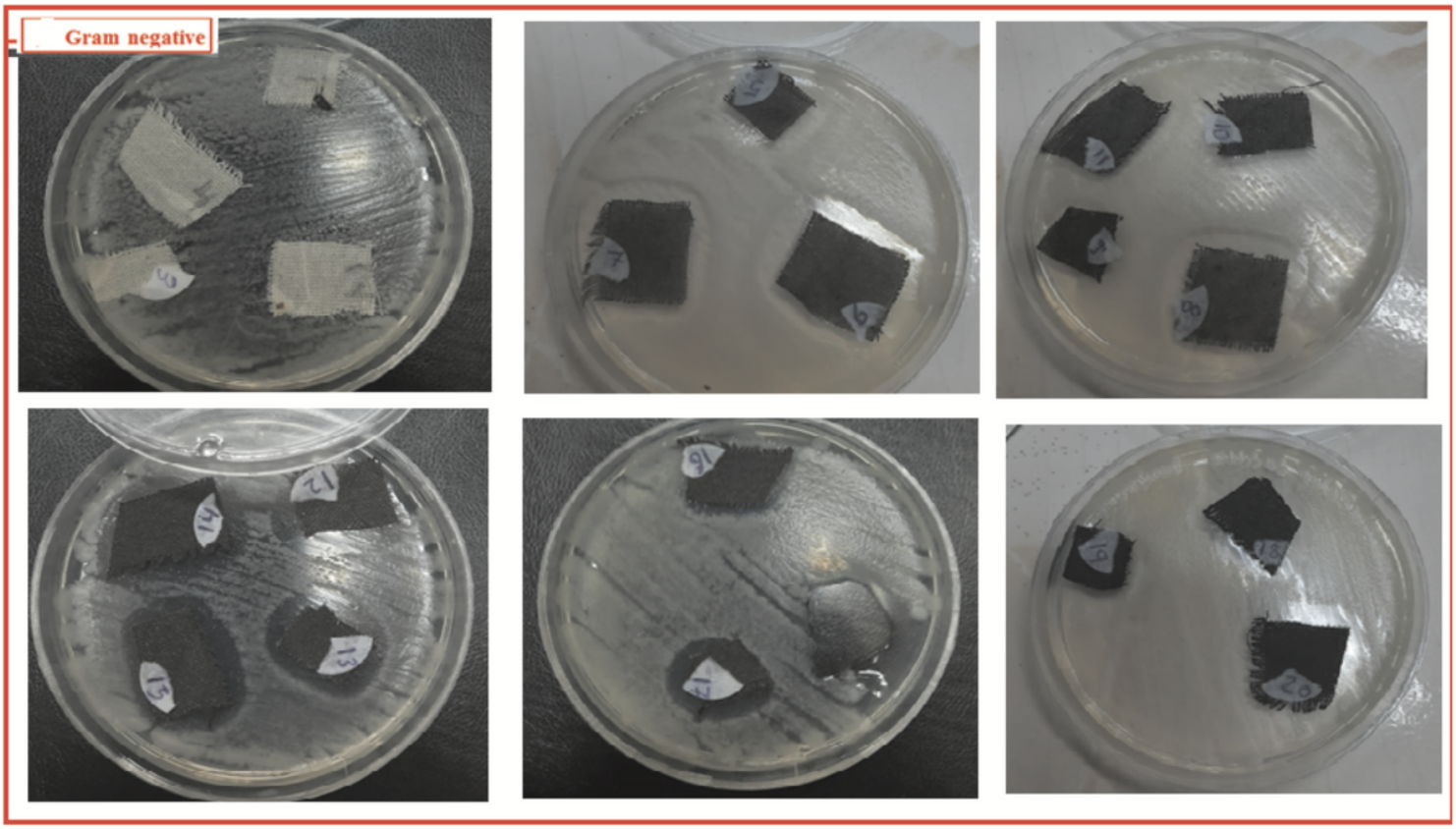

Figure 13

The antibacterial activities of the unmodified and modified cotton fabrics by CMC/PEG/EG with Ag/ different ratios CuO NPs: for code samples (1, 2, 3 and 4) of the unmodified cotton fabrics / CMC/PEG/EG, (5, 6, 7 and 8) of the modified cotton fabrics by CMC/PEG/EG/ (0.006%) Ag/ (0.012%) CuO, (9, 10, 11 and 12) of the modified cotton fabrics by CMC/PEG/EG/ (0.006%) Ag/ (0.5%) CuO, (13, 14, 15 and 16) of the modified cotton fabrics by CMC/PEG/EG/ (0.006%) Ag/ (1%) CuO, and (17, 18, 19 and 20) of the modified cotton fabrics by CMC/PEG/EG/ (0.006%) Ag/ (2%) CuO at various EB radiation doses against Gram -ve Bacteria

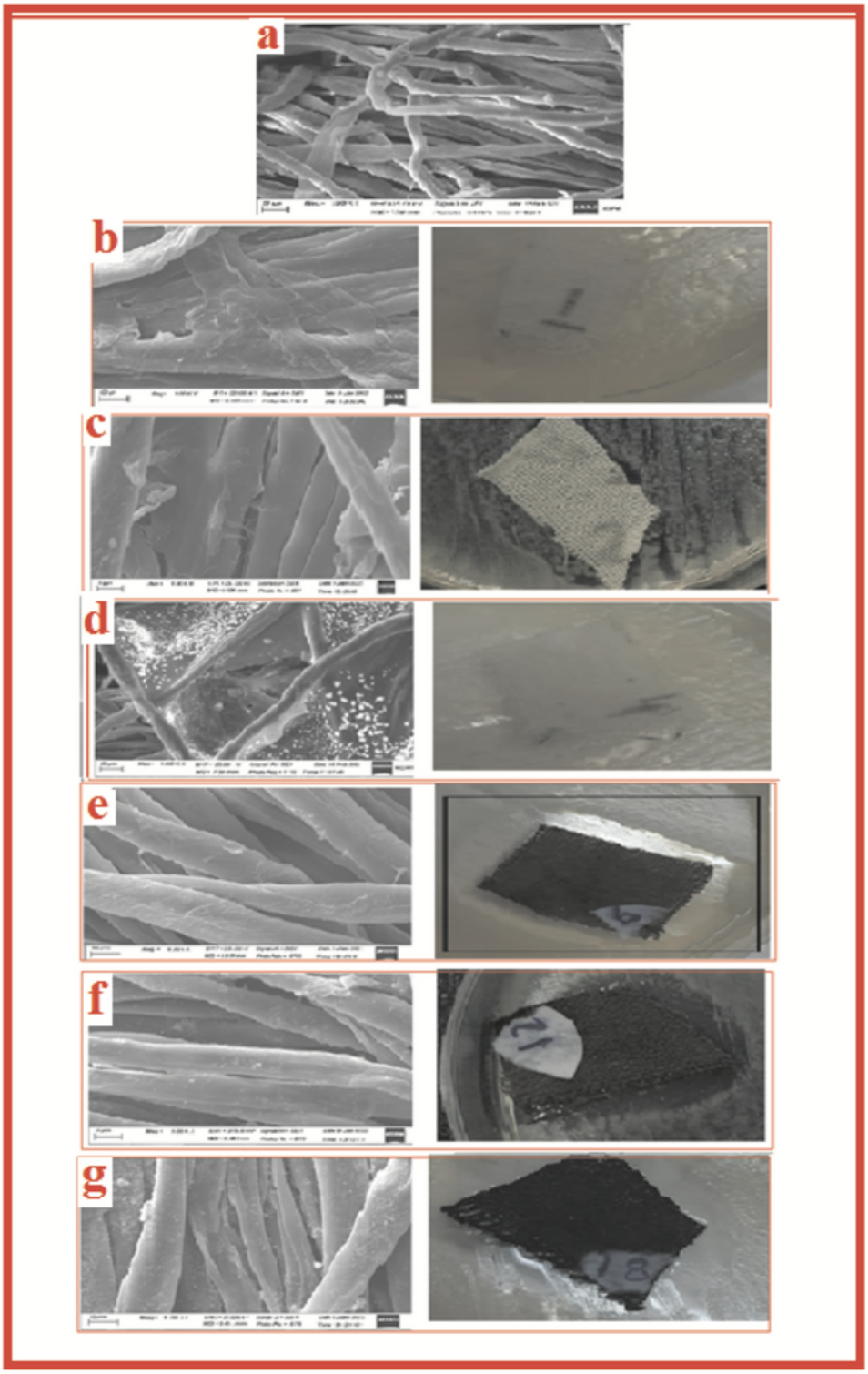

Figure 14

SEM images and dishes of cotton fabrics unmodified and modified against bacteria: (A) pure cotton fabrics without bacteria, (B) cotton fabrics by padding in CMC/PEG/EG at 0 kGy, (C) cotton fabrics by padding in CMC/PEG/EG at 5 kGy, (D) cotton fabrics by padding in CMC/PEG/EG at 25 kGy, (E) cotton fabrics by padding in CMC/PEG/EG containing (0.006%) Ag/ (0.012%) CuO at 5 kGy, (F) cotton fabrics by

padding in CMC/PEG/EG containing (0.006%) Ag/ (0.5%) CuO at 25 kGy and (G) cotton fabrics by padding in CMC/PEG/EG containing (0.006%) Ag/ (2%) CuO at 5 kGy

Supplementary Files

This is a list of supplementary files associated with this preprint. Click to download.

- Highlights.docx